Regulatory Subunit B′γ of Protein Phosphatase 2A Prevents Unnecessary Defense Reactions under Low Light in Arabidopsis[1][W][OA]

Andrea Trotta, Michael Wrzaczek, Judith Scharte, Mikko Tikkanen[2], Grzegorz Konert, Moona Rahikainen, Maija Holmström, Hanna-Maija Hiltunen[3], Stephan Rips, Nina Sipari, Paula Mulo, Engelbert Weis, Antje von Schaewen, Eva-Mari Aro, and Saijaliisa Kangasjärvi*

Department of Biochemistry and Food Chemistry, University of Turku, FI–20014 Turku, Finland (A.T., M.T., G.K., M.R., M.H., H.-M.H., P.M., E.-M.A., S.K.); Department of Biosciences, University of Helsinki, FI–00014 Helsinki, Finland (M.W., N.S.); and Institute for Botany, University of Munster, DE–48149 Munster, Germany (J.S., H.-M.H., S.R., E.W., A.v.S.)

Light is an important environmental factor that modulates acclimation strategies and defense responses in plants. We explored the functional role of the regulatory subunit B′γ (B′γ) of protein phosphatase 2A (PP2A) in light-dependent stress responses of Arabidopsis (*Arabidopsis thaliana*). The predominant form of PP2A consists of catalytic subunit C, scaffold subunit A, and highly variable regulatory subunit B, which determines the substrate specificity of PP2A holoenzymes. Mutant leaves of knockdown *pp2a-b′γ* plants show disintegration of chloroplasts and premature yellowing conditionally under moderate light intensity. The cell-death phenotype is accompanied by the accumulation of hydrogen peroxide through a pathway that requires CONSTITUTIVE EXPRESSION OF PR GENES5 (CPR5). Moreover, the *pp2a-b′γ cpr5* double mutant additionally displays growth suppression and malformed trichomes. Similar to *cpr5*, the *pp2a-b′γ* mutant shows constitutive activation of both salicylic acid- and jasmonic acid-dependent defense pathways. In contrast to *cpr5*, however, *pp2a-b′γ* leaves do not contain increased levels of salicylic acid or jasmonic acid. Rather, the constitutive defense response associates with hypomethylation of DNA and increased levels of methionine-salvage pathway components in *pp2a-b′γ* leaves. We suggest that the specific B′γ subunit of PP2A is functionally connected to CPR5 and operates in the basal repression of defense responses under low irradiance.

Dynamic adjustments in developmental programs and metabolic processes allow plants to cope with biotic and abiotic stress factors that continuously alternate in nature. Among environmental cues, the availability of light is one of the key factors that modulate the acclimation strategies and defense reactions in plants. The light-dependent adaptive responses are closely connected with metabolic pathways of chloroplasts, which are highly responsive to environmental fluctuations and known to carry out important signaling functions in various stress responses in plants (Kangasjärvi et al., 2009). Besides their importance in light acclimation, chloroplasts also mediate responses to wounding, air pollutants, and infection by various types of plant pathogens (Dat et al., 2000; Kachroo et al., 2003; Joo et al., 2005; Kariola et al., 2005; Mühlenbock et al., 2008). However, the final acclimation response is an outcome of cross talk among organellar signals and cytoplasmic networks, including those resulting from photoperiodic and hormonal regulation (Queval et al., 2007; Griebel and Zeier, 2008).

Controlled protein dephosphorylation by Ser/Thr protein phosphatase 2A (PP2A) family members is a crucial mechanism that regulates various signaling events in plants (DeLong, 2006). The predominant form of PP2A is trimeric, consisting of a catalytic subunit C, a scaffold subunit A, and a highly variable regulatory subunit B. The genome of Arabidopsis (*Arabidopsis thaliana*) contains five genes encoding PP2A-C subunits, three functionally distinct A subunits (PP2A-A1, PP2A-A2, and PP2A-A3), and 17 largely uncharacterized B subunits, which are further divided into B, B′, and B″ subfamilies. Notably, the B subunit has a crucial function for PP2A activity, since it influ-

[1] This work was supported by the Finnish Cultural Foundation, the Academy of Finland (project nos. 218157, 130595, 8130595, 118637, 130075, and 141121), the German Research Foundation (grant no. DFG Scha 541/11), and a Helsinki University postdoctoral research grant. Funding for the SIGnAL indexed insertion mutant collection and the cDNA/ORFeome collection was provided by the National Science Foundation.

[2] Present address: Departments of Plant Biology and Molecular Biology, University of Geneva, 1211 Geneva 4, Switzerland.

[3] Present address: Institute of Biology, Humboldt University Berlin, DE–10115 Berlin, Germany.

* Corresponding author; e-mail saijaliisa.kangasjarvi@utu.fi.

The author responsible for distribution of materials integral to the findings presented in this article in accordance with the policy described in the Instructions for Authors (www.plantphysiol.org) is: Saijaliisa Kangasjärvi (saijaliisa.kangasjarvi@utu.fi).

[W] The online version of this article contains Web-only data.

[OA] Open Access articles can be viewed online without a subscription.

www.plantphysiol.org/cgi/doi/10.1104/pp.111.178442

ences the structural conformation of PP2A, which in turn determines the target specificity of the PP2A holoenzyme (Farkas et al., 2007). The large number of isoforms for each subunit provides extensive variability of combinations for the trimeric PP2A holoenzyme, which allows versatile but highly specific functions for PP2A in the dephosphorylation of various target proteins.

Experiments with the phosphatase inhibitor okadaic acid have implicated a role for PP2A-mediated protein dephosphorylation in a range of developmental programs and acclimation processes, including seed germination (Chang et al., 1999), cold acclimation (Monroy et al., 1998), and wounding (Rojo et al., 1998). Okadaic acid, however, does not specifically inhibit PP2A, and more detailed information concerning the specific functions of individual A, B, and C subunits of PP2A has arisen from studies using mutant approaches. PP2A-A1 was first identified as ROOTS CURL IN NAPHTHYLPHTHALAMIC ACID1 (RCN1) and found to regulate basipetal auxin transport (Rashotte et al., 2001). Subsequent analysis of *rcn1* null mutants demonstrated that the absence of RCN1 renders plants insensitive to blue light, abscisic acid, and jasmonic acid (JA) signaling in stomatal closure (Kwak et al., 2002; Saito et al., 2008; Tseng and Briggs, 2010) and blocks the biosynthesis of ethylene (ET; Larsen and Cancel, 2003). Such multiple phenotypic effects of *rcn1* suggest that, in wild-type plants, the specific targets for RCN1-containing PP2A complexes may in fact be determined by the identity of the regulatory B subunit in the PP2A holoenzyme.

Of the regulatory B subunits, the B″-type PP2A subunit TONNEAU2 was found to regulate the dynamic organization of the cortical cytoskeleton (Camilleri et al., 2002), whereas a metabolic role for B55-type subunits α and β in the activation of nitrate reductase was recently reported (Heidari et al., 2011). Lately, vital roles for PP2A in the regulation of cell elongation and growth through brassinosteroid signaling (Tang et al., 2011) and the TARGET OF RAPAMYCIN (TOR) pathway (Ahn et al., 2011) were elucidated, and a role for the catalytic PP2A-C2 subunit as a negative regulator of abscisic acid signaling has also been demonstrated (Pernas et al., 2007).

In tobacco (*Nicotiana tabacum*), silencing of catalytic PP2A subunits induced the constitutive expression of pathogenesis-related (PR) genes and accelerated cell death in response to bacterial and fungal elicitors (He et al., 2004), demonstrating the importance of catalytic PP2A activity in the regulation of defense reactions in plants. Mutants with spontaneous activation of defense-related genes and/or induction of cell death have also been identified in Arabidopsis mutant screens (Lorrain et al., 2003). A vast number of these mutants are sensitive to high light and show enhanced hypersensitive reaction-like cell death upon light-induced reduction of the photosynthetic electron transport chain and/or accumulation of reactive oxygen species (ROS) in chloroplasts (Lorrain et al., 2003). How chloroplasts contribute to defense signaling under low light intensities, however, remains poorly understood.

In animal cells, the regulation of cell death cascades involves B′-type regulatory subunits that target the trimeric PP2A holoenzyme to specific phosphoproteins in a highly coordinated manner (Li et al., 2002). Here, we have identified a B′γ-type regulatory subunit of PP2A that regulates disease resistance and the maintenance of chloroplast integrity under moderately low light intensity. Knockdown *pp2a-b′γ* mutant plants show constitutive activation of defense responses, which correlates with the disintegration of chloroplasts and finally the age-dependent formation of yellowing patches when plants grow under moderate light. The cell-death phenotype is accompanied by the accumulation of ROS through a pathway that requires the activity of CONSTITUTIVE EXPRESSION OF PR GENES5 (CPR5), another component that modulates the attainment of stress tolerance under low irradiance levels in Arabidopsis.

RESULTS

Identification of Knockdown *pp2a-b′γ* Mutant Plants and Characteristics of PP2A-B′γ

We took a reverse genetic approach to identify components that specifically modulate the capacity of plants to tolerate different light intensities. The *pp2a-b′γ* mutant, deficient in a specific regulatory B′γ subunit of PP2A, was chosen for further analysis, since it showed an intriguing phenotype with wrinkled leaves, stunted growth, delayed flowering, and age-dependent formation of yellowing lesions when grown under a moderate growth light intensity of 130 μmol photons $m^{-2} s^{-1}$ (Fig. 1A; Table I). The premature wilting was reflected by reduced seed production capacity of the *pp2a-b′γ* mutant plants (Table I). Notably, a knockout line deficient in the PP2A-B′ζ (At3g21650) protein, whose amino acid sequence is 83% identical with that of PP2A-B′γ, revealed no visual phenotype (Supplemental Fig. S1).

Sequencing over the T-DNA border of *pp2a-b′γ* plants revealed an insertion in the 5′ untranslated region of the *PP2A-B′γ* gene (At4g15415; Fig. 1B). Analysis by quantitative real-time PCR confirmed lower *PP2A-B′γ* transcript abundance in *pp2a-b′γ* mutants (0.41-fold ± 0.19-fold compared with *PP2A-B′γ* levels in the wild type; Fig. 1A). No RNA interference lines or additional T-DNA lines with insertion in the transcribed region of At4g15415 were available for parallel analysis. Thus, to genetically complement the mutation, we introduced the *PP2A-B′γ* protein-coding sequence under the 35S cauliflower mosaic virus promoter into *pp2a-b′γ*. In this complementation line, somewhat variable levels of *PP2A-B′γ* mRNA (2.2-fold ± 1.0-fold compared with wild-type levels) were detected, but the growth rate was restored and no premature yellowing was observed (Fig. 1A).

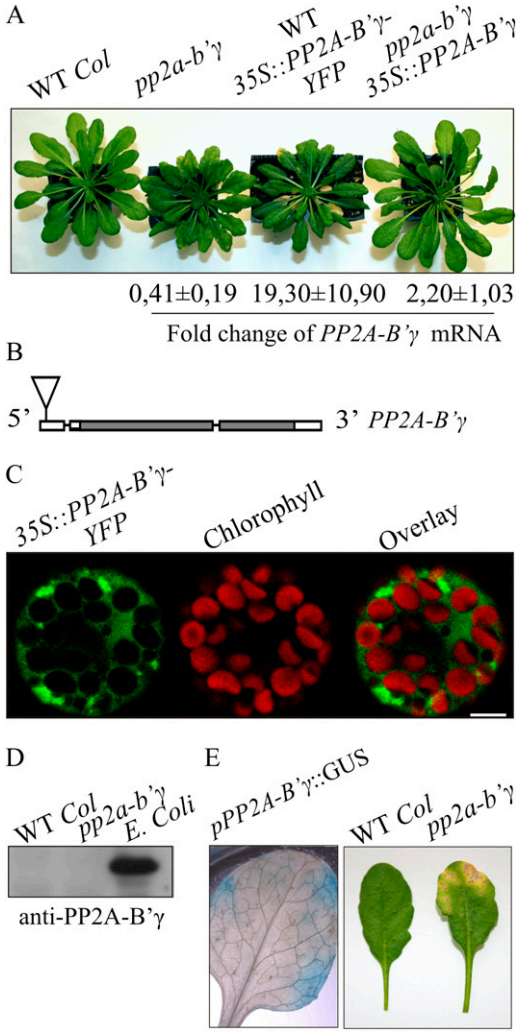

Figure 1. Identification of the knockdown *pp2a-b′γ* mutant and characteristics of PP2A-B′γ. A, Visual phenotypes of 5-week-old wild-type (WT Col) plants, the *pp2a-b′γ* mutant, a line expressing 35S-driven expression of PP2A-B′γ-YFP in the wild-type background, and a *pp2a-b′γ* line complemented by 35S-driven expression of the *PP2A-B′γ* gene. The fold change of *PP2A-B′γ* mRNA accumulation as compared with the wild type is shown below. B, Molecular structure and T-DNA insertion site of the *PP2A-B′γ* gene (At4g15415; SALK_039172). The T-DNA insertion site is indicated with the triangle, introns are indicated with lines, and the gray and white boxes represent exons and untranslated regions, respectively. C, Transient expression of *35S::PP2A-B′γ-YFP* in Arabidopsis protoplasts to demonstrate the subcellular localization of PP2A-B′γ . Fluorescence from YFP is shown in green, and chlorophyll autofluorescence is shown in red. Bar = 5 μm. D, Immunoblot with anti-PP2A-B′γ antibody of total leaf extracts isolated from the wild type and *pp2a-b′γ*. Immunoresponse from a cellular lysate of *E. coli* heterologously expressing PP2A-B′γ-6xHIS is shown in parallel. E, Promoter-driven GUS analysis demonstrating activity of the *PP2A-B′γ* gene in leaves under growth light conditions (130 μmol photons m^{-2} s^{-1}). A photograph depicting the yellowing lesion on a 6-week-old *pp2a-b′γ* mutant leaf is shown in parallel.

It is worth noting that 35S-driven expression of a *PP2A-B′γ-YFP* (for yellow fluorescent protein) fusion construct in *pp2a-b′γ* failed to complement the mutation (data not shown). On the other hand, overexpression of the *PP2A-B′γ-YFP* fusion construct in wild-type Arabidopsis plants resulted in a yellowing phenotype, which highly resembled that of the *pp2a-b′γ* mutant (Fig. 1A). This was likely due to a dominant-negative effect on the PP2A complex and not due to cosuppression of *PP2A-B′γ*, since the abundance of *PP2A-B′γ* mRNA in the line expressing *PP2A-B′γ-YFP* was found to be 19-fold higher than that of the wild-type plants (Fig. 1A). Among hundreds of transgenic seedlings screened for the presence of PP2A-B′γ-YFP, only a few individuals showed YFP fluorescence in cotyledons, but all these individuals failed in development and wilted before the appearance of the first true leaves (data not shown). Imaging of Arabidopsis protoplasts transiently overexpressing the fusion construct, however, revealed PP2A-B′γ-YFP fluorescence predominantly in the cytoplasm (Fig. 1C), as also recently reported by Matre et al. (2009).

Similar to attempts to visualize PP2A-B′γ-YFP, detection of PP2A-B′γ by immunoblotting using an antibody raised against PP2A-B′γ repeatedly failed (Fig. 1D), presumably due to low abundance of PP2A-B′γ. Indeed, when PP2A-B′γ was produced in bacteria, the protein could be detected by anti-PP2A-B′γ antibodies (Fig. 1D). To obtain insights into the pattern of *PP2A-B′γ* gene expression, the *uidA* (GUS reporter) gene was introduced into wild-type Arabidopsis plants and expressed under the *PP2A-B′γ* promoter consisting of a 2.8-kb region upstream of the translational start codon on the *PP2A-B′γ* coding sequence. Subsequent GUS analyses demonstrated that in rosette leaves, the *PP2A-B′γ* promoter was active in patches that highly resembled the yellowing areas, which developed on *pp2a-b′γ* mutant leaves upon aging (Fig. 1E). Within these peripheral patches, also the veins showed *PP2A-B′γ* promoter-driven GUS activity. These results indicate that PP2A-B′γ is a low-abundance signaling component that is specifically expressed in limited areas in leaves.

Degeneration of Cellular Components in Visually Healthy *pp2a-b′γ* Leaves

Microscopic examination revealed distinct abnormalities in the mesophyll tissue of *pp2a-b′γ* plants well before visual detection of yellowing patches under

Table I. *Flowering time, seed production capacity, and CO_2 assimilation rate of wild type and pp2a-b′γ mutant plants grown at 130 μmol photons m^{-2} s^{-1}/22°C*

n = 15 for flowering time, *n* = 3 for seed production, and *n* = 6 for photosynthesis activity measurement. The asterisks denote that the *t* test *P* value is below 0.05.

Plant Type	Floral Induction	Seed Production	Photosynthetic Activity
	d	*mg plant*$^{-1}$	*μmol* CO_2 m^{-2} s^{-1}
Wild type	63 ± 4	352 ± 44	2.6 ± 0.24
pp2a-b′γ	77 ± 6*	223 ± 25*	2.4 ± 0.33

moderate light intensity. In the palisade parenchyma cells of *pp2a-b′γ* leaves, 28% of the chloroplasts were roundish and/or showed loosening of the photosynthetic membranes (Fig. 2A), which is a phenomenon normally observed at early phases of senescence. In wild-type leaves, such degrading chloroplasts were not observed (Fig. 2B). In the spongy mesophyll tissue of *pp2a-b′γ*, 64% of chloroplasts showed distinct symptoms of degeneration, and some of the chloroplasts contained thylakoid-free extrusions (Fig. 2C). Intriguingly, the spongy mesophyll tissue of *pp2a-b′γ* also contained separate cells with a curving plasma membrane indicative of cell death in this specific cell type (Fig. 2C). Confocal microscopy imaging of propidium iodide-stained leaf tissue also revealed separate cells with extensive cell shrinkage and intense propidium iodide staining of nuclei in *pp2a-b′γ* leaves (Fig. 2D), indicative of cell death. In the remaining thylakoid membranes, however, the photosynthetic membrane protein complexes remained intact (Fig. 2E), and the net CO_2 assimilation did not significantly differ between wild-type and *pp2a-b′γ* plants either (Table I). Collectively, the knockdown of *PP2A-B′γ* promoted senescence-like symptoms, suggesting that the PP2A activity mediated by B′γ is required for the maintenance of cellular integrity in Arabidopsis leaves.

Comparative Transcript Profiling of *pp2a-b′γ* and Wild-Type Plants

Comparative transcript profiling of *pp2a-b′γ* and wild-type plants grown for 4 weeks under moderate light intensity revealed constitutively elevated transcript levels of defense-related genes in *pp2a-b′γ* plants (Supplemental Table S1). The most distinct response was a several-fold increase in expression of salicylic acid (SA)-related components, including *PATHOGENESIS-RELATED1* (*PR1*), *PR5*, *ISOCHORISMATE SYNTHASE1*, *PHYTOALEXIN-DEFICIENT4*, and *ENHANCED DISEASE SENSITIVITY1* (*EDS1A* and *EDS1B*; Supplemental Table S1). Furthermore, *pp2a-b′γ* plants showed higher expression levels of resistance (R) genes encoding intracellular Toll-interleukin 1 nucleotide-binding Leu-rich repeat receptors, coiled-coil nucleotide-binding Leu-rich repeat receptors, as well as Leu-rich repeat-class disease resistance proteins (Supplemental Table S1). Finally, the constitutive defense response of *pp2a-b′γ* manifested as enhanced expression of genes coding for cytosolic *h*-type thioredoxins, chitinases, glutathione *S*-transferases, and other defense-related genes (Supplemental Tables S1 and S2).

Besides SA-related signaling components, *pp2a-b′γ* plants also showed higher expression levels of genes related to the biosynthesis of JA or ET compared with the wild type (Supplemental Table S2). Two genes coding for 1-aminocyclopropane-1-carboxylate oxidases, three genes coding for allene oxide synthases, lipoxygenase 2, and 12-oxophytodienoate reductase were induced in *pp2a-b′γ* as compared with wild-type plants (Supplemental Table S1). Also, the ET/JA marker genes encoding PLANT DEFENSIN1.2 and a Tyr aminotransferase (At2g24850; Penninckx et al., 1998) were induced in the *pp2a-b′γ* mutant (Supplemental Table S1).

Three general ROS markers, *At1g19020*, *At2g43510*, and *At1g57630* (Gadjev et al., 2006), showed slightly

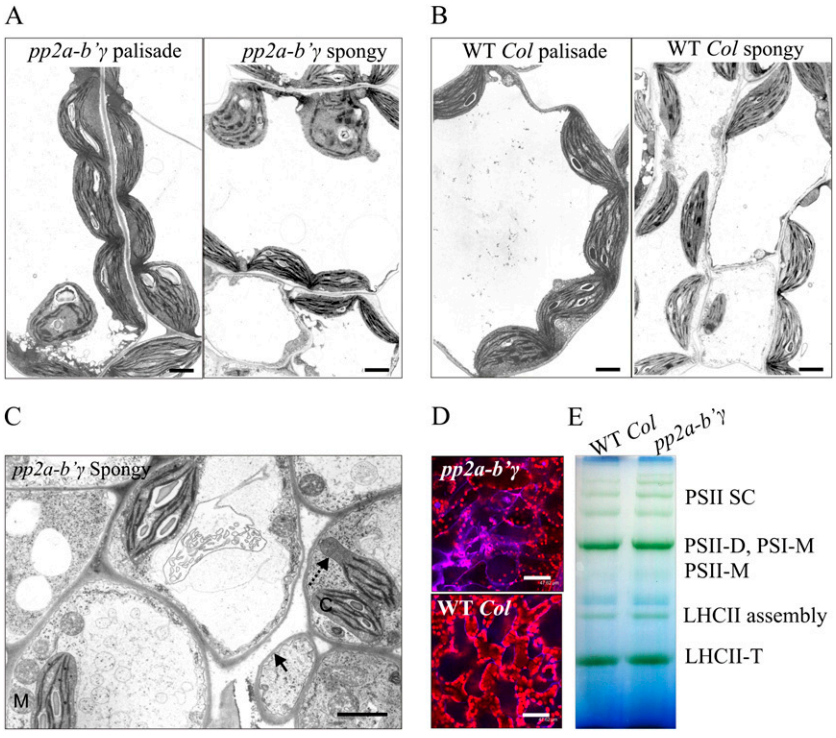

Figure 2. Structural properties of visually presymptomatic *pp2a-b′γ* leaves. A and B, Ultrastructural properties of mesophyll cells in *pp2a-b′γ* and wild-type (WT Col) plants. The electron micrographs are representative images of palisade mesophyll and spongy mesophyll tissues. Bars = 2 μm. C, Electron micrograph depicting abnormalities in the spongy mesophyll tissue of *pp2a-b′γ* leaves. Wrinkled plasma membrane indicative of the initiation of cell death and a homogenous extrusion of chloroplast are indicated with the solid and dashed arrow, respectively. C, Chloroplast; M, mitochondrion. Bar = 2 μm. D, Confocal microscopy images of propidium iodide-stained leaf tissues demonstrating the onset of cell death in *pp2a-b′γ* leaves. Bars = 47.62 μm. E, Blue native gel demonstrating a similar pattern of photosynthetic thylakoid protein complexes in wild-type and *pp2a-b′γ* leaves. D, Dimer; LHCII, light-harvesting antenna of PSII; M, monomer; SC, supercomplex; T, trimer.

elevated transcript levels in *pp2a-b′γ* plants (Supplemental Table S1). Among antioxidant enzymes, transcript levels for iron-superoxide dismutase, chloroplast NADPH-dependent thioredoxin reductase, glutathione peroxidase 7, and catalase 2 were lowered in *pp2a-b′γ* (Supplemental Table S1). In contrast, transcript levels for two genes encoding chloroplastic monodehydroascorbate reductases, three encoding Met sulfoxide reductases, five encoding thioredoxin family proteins, and one for catalase 3 (SEN2) were higher in *pp2a-b′γ* as compared with wild-type plants (Supplemental Table S1). Moreover, slightly increased expression of cell death antagonists, including *At5g47120* and *At3g16770*, which have a role in the suppression of Bcl2-associated X protein-induced programmed cell death, was also observed in *pp2a-b′γ* (Supplemental Table S1). Altogether, *pp2a-b′γ* plants show a constitutive reprogramming of transcript accumulation for ROS-, SA-, and JA/ET-responsive genes.

Phenotypic Characteristics of *pp2a-b′γ*, *cpr5*, and *pp2a-b′γ cpr5* Double Mutant Plants under Different Light Intensities

Next, we compared the transcript profiles of 4-week-old *pp2a-b′γ* and wild-type plants grown under normal growth light (130 μmol photons m^{-2} s^{-1}) or under high light (800 μmol photons m^{-2} s^{-1}). Differences in transcript profiles of the wild type and *pp2a-b′γ* were particularly pronounced when the plants were grown under normal growth light conditions, where differential regulation (greater than 1.5-fold and $P < 0.05$) of 645 genes was observed (Fig. 3; Supplemental Table S2). Of these, 478 showed elevated transcript levels in *pp2a-b′γ* compared with the wild type (Fig. 3A). In high-light-grown *pp2a-b′γ* plants, the number of differentially expressed genes was 317, of which 235 showed increased transcript levels (Fig. 3A). Associated with a partial dampening of defense gene expression (Supplemental Table S2), also the yellowing phenotype of *pp2a-b′γ* could be rescued upon growth under high light (Fig. 3B).

Similar to *pp2a-b′γ*, the lesion-mimic mutant *cpr5* also showed up-regulation of SA and JA marker genes and underwent premature senescence when grown under moderate growth light conditions (Clarke et al., 2000). Thus, we tested the genetic interaction between *pp2a-b′γ* and *cpr5*. Parallel growth of *cpr5* and *pp2a-b′γ* revealed that the onset of yellowing occurred somewhat earlier in *cpr5*. With respect to yellowing, the *pp2a-b′γ cpr5* double mutant resembled *cpr5*. However, the growth rate of *pp2a-b′γ cpr5* was reduced as compared with either of the parental lines (Fig. 3B). When grown under high light intensity, the growth rate of *pp2a-b′γ*, *cpr5*, and the *pp2a-b′γ cpr5* plants was partly restored (Fig. 3B).

During characterization of the mutant phenotypes, we noted that the apparent functional connection between PP2A-B′γ and CPR5 is reflected also by aberrant trichomes. The *cpr5* mutant has a distinct trichome phenotype with two branches, whereas wild-type trichomes generally have three branches (Kirik et al., 2001; Fig. 3B). The *pp2a-b′γ* plants commonly showed trichomes with three or four branches, whereas the *pp2a-b′γ cpr5* double mutant revealed an additive malformation, displaying branchless trichomes of severely reduced cell size (Fig. 3B).

Whereas diaminobenzidine (DAB) staining showed increased accumulation of hydrogen peroxide (H_2O_2), particularly in the oldest leaves of *pp2a-b′γ*, no distinct DAB staining was observed in *cpr5* or the *pp2a-b′γ cpr5* double mutant (Fig. 3B). Furthermore, after long-term growth under high light, none of the plants revealed distinct H_2O_2 accumulation (Fig. 3B). The differential ROS accumulation in the different mutant backgrounds prompted us to use the methyl viologen (MV) test to examine the sensitivity of visually healthy *pp2a-b′γ*, *cpr5*, and *pp2a-b′γ cpr5* plants to photooxidative stress. MV extracts electrons from PSI and then reacts with molecular oxygen to produce superoxide (O_2^-) and subsequently H_2O_2 in chloroplasts. Plants were sprayed with 50 μM MV, illuminated under moderate growth light for 6 h, and analyzed for the extent of ion leakage. Clearly, cell death in *pp2a-b′γ* plants was accelerated by MV treatment as compared with wild-type plants (Fig. 3C). In contrast, neither *cpr5* nor the *pp2a-b′γ cpr5* double mutant showed any enhanced sensitivity to MV-induced photooxidative stress (Fig. 3C).

Disease resistance is generally connected with increased levels of SA and JA in leaves. Parallel analysis of wild-type, *pp2a-b′γ*, *cpr5*, and *pp2a-b′γ cpr5* plants revealed increased levels of SA and to a lesser extent also JA in *cpr5* and *pp2a-b′γ cpr5* plants. Notably, *pp2a-b′γ* plants revealed no changes in hormone levels as compared with wild-type plants (Fig. 3D).

Proteomic Analysis of *pp2a-b′γ* and Wild-Type Leaves

To investigate the proteomic profile of *pp2a-b′γ* leaves, oligomeric protein complexes in total soluble leaf extracts of *pp2a-b′γ* and wild-type plants were separated by clear native (CN)-PAGE followed by SDS-PAGE in the second dimension (Fig. 4A). For sensitive visualization of spot intensities, gels were first stained with SYPRO Ruby and thereafter silver stained for identification of spots of interest by mass spectrometry (Table II).

Imaging of SYPRO-stained two-dimensional (2D) gels revealed 11 proteins with consistently higher abundance in *pp2a-b′γ* soluble leaf extracts as compared with wild-type plants (Fig. 4A; Table II). These proteins were assigned to different functional groups, including defense and stress, amino acid metabolism, Met-salvage pathway, and the nonoxidative branch of the pentose phosphate pathway (Table II). The identified defense- and stress-related proteins included myrosinase thioglucoside glucohydrolase 1 (TGG1), carbonic anhydrase 1 (CA1), glutathione *S*-transferase F2 (AtGSTF2), and the chloroplastic copper/zinc

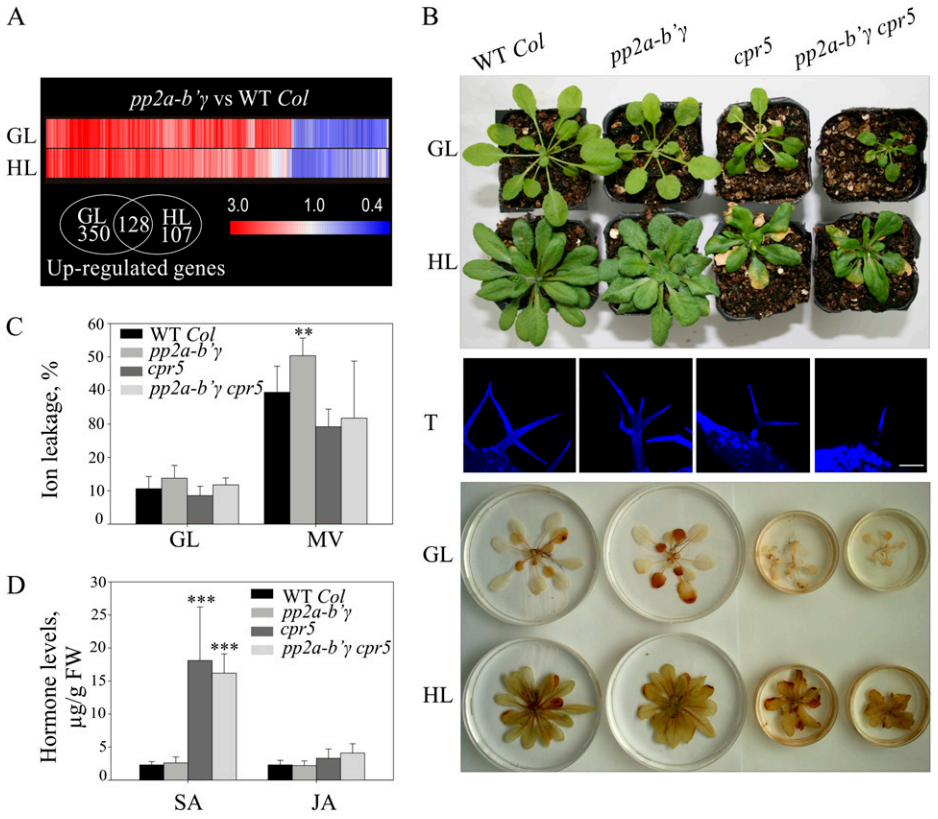

Figure 3. Characteristics of *pp2a-b′γ*, *cpr5*, the *pp2a-b′γ cpr5* double mutant, and wild-type plants. A, Clustering of genes differentially expressed between *pp2a-b′γ* mutant and wild-type (WT Col) plants under normal growth light conditions (GL; 130 μmol photons m^{-2} s^{-1}) or after growth under high light (HL; 800 μmol photons m^{-2} s^{-1}). Genes that showed statistically significant (Student's *t* test; $P < 0.05$) differences in expression of at least 1.5-fold under either GL or HL are presented. The Venn diagram demonstrates the number of up-regulated genes in *pp2a-b′γ* mutant plants under GL and HL. B, Visual phenotypes and accumulation of H_2O_2 in *pp2a-b′γ*, *cpr5*, and the *pp2a-b′γ cpr5* double mutant after a 4-week growth period under GL and HL. For visualization of H_2O_2, rosettes were floated on 0.1% DAB under GL conditions for 2 h. The accumulation of H_2O_2 is visualized as a brown precipitate on the leaves. Projections of sequential confocal microscopy images of Hoechst-stained trichomes (T) of the wild type, *pp2a-b′γ*, *cpr5*, and the *pp2a-b′γ cpr5* double mutant are shown between the photographs. Bar = 100 μm. C, Sensitivity to MV-induced photooxidative stress. Plants were sprayed with 50 μM MV and illuminated under 130 μmol photons m^{-2} s^{-1} for 6 h prior to measurement of ion leakage from the leaves. Control samples were illuminated under normal GL conditions. The values are means ± SD ($n = 9$). ** $P < 0.05$ by Student's *t* test. D, Levels of SA and JA in *pp2a-b′γ*, *cpr5*, and the *pp2a-b′γ cpr5* double mutant after a 4-week growth period under GL. *** $P < 0.005$ by Student's *t* test. FW, Fresh weight.

superoxide dismutase (CSD2; Table II). TGG1 catalyzes the release of toxic compounds from glucosinolates upon biotic challenge, whereas CA1 was identified in a screen for SA-binding proteins and is connected with the onset of hypersensitive cell death in tobacco (Slaymaker et al., 2002). AtGSTF2, on the other hand, is rapidly induced by different stimuli, including MV, SA, ET, and pathogen attack (Smith et al., 2003; Dixon and Edwards, 2010), and CSD2 is a key scavenger of O_2^- in the chloroplast. However, also among the metabolic enzymes up-regulated in *pp2a-b′γ*, cytoplasmic Gln synthase 1 (AtGLN1;1) and chloroplastic transketolase (TKL) contribute to defense responses and have been shown to increase in abundance in response to pathogen infection (Liu et al., 2010). Furthermore, ONSET OF LEAF DEATH3 (OLD3), the cytosolic Cys biosynthesis enzyme *O*-acetyl-Ser(thiol) lyase, maintains cellular thiol levels and has a function in the regulation of cell death (Shirzadian-Khorramabad et al., 2010).

AtGSTF2 and CSD2 comigrated on the gels and were identified with high scores from the same spot (Fig. 4A; Table II). Thus, increase in the steady-state level of CSD2 in *pp2a-b′γ* was confirmed by immunoblotting (Fig. 4B). Regulation of CSD2 function involves the binding of aconitase (ACO) in the 5′ untranslated region of *CSD2* mRNA (Moeder et al., 2007). Intriguingly, even though ACO was not identified through the proteomic approach, immunoblotting revealed increased steady-state levels of ACO in *pp2a-b′γ* as compared with wild-type plants (Fig. 4B). By contrast, the level of fructose bisphosphate aldolase (FBA) showed no major changes between *pp2a-b′γ* and wild-type plants (Fig. 4B).

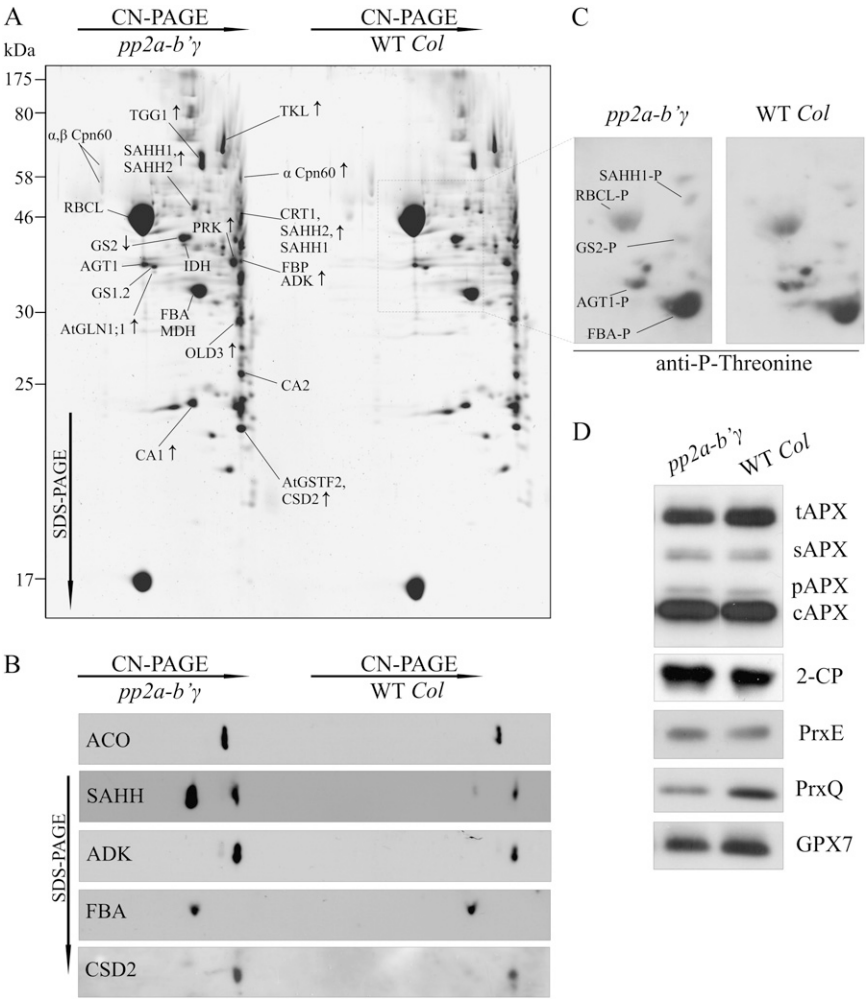

Figure 4. Proteomic analysis of *pp2a-b′γ* leaves. A, Representative SYPRO-stained 2D gel depicting proteins in the total foliar soluble fractions isolated from *pp2a-b′γ* and wild-type (WT Col) plants. Oligomeric complexes were separated by CN-PAGE followed by SDS-PAGE in the second dimension. The proteins were identified by in-gel trypsin digestion and subsequent analysis by nano-HPLC electrospray ionization-quadrupole-time-of-flight MS/MS. Protein spots showing higher or lower intensity in *pp2a-b′γ* as compared with the wild type are indicated by arrows. Details concerning the identified proteins and phosphopeptides are presented in Table II. B, Immunoblots of 2D gels demonstrating increased steady-state levels of ACO, SAHH (isoforms 1 and 2 in both of the spots), ADK, and CSD2 in the *pp2a-b′γ* mutant as compared with wild-type plants. Fru bisphosphate aldolase (FBA) is shown as a control, as it showed no differences between the lines. C, Phosphoproteins of *pp2a-b′γ* and wild-type soluble leaf extracts as detected from 2D CN-PAGE by immunoblotting with anti-P-Thr antibody. The phosphoproteins were identified based on relative locations to Rubisco subunits on the gel and on the presence of phosphopeptides in the MS/MS spectra as presented in Table II. The corresponding area on a SYPRO-stained 2D gel is indicated with a box in A. D, Steady-state levels of antioxidant enzymes in *pp2a-b′γ* mutant and wild-type plants. tAPX, Thylakoid ascorbate peroxidase (APX); sAPX, stromal APX; pAPX, peroxisomal APX; cAPX, cytoplasmic APX; 2-CP, chloroplastic 2-Cys peroxiredoxins A and B; PrxE, peroxiredoxin IIE; PrxQ, peroxiredoxin Q; GPX7, glutathione peroxidase 7.

Two components of the Met-salvage pathway, *S*-adenosyl-L-homocysteine hydrolase (SAHH) and adenosine kinase (ADK), were also found increased in abundance in *pp2a-b′γ* as compared with wild-type plants (Fig. 4A; Table II). This result was confirmed by immunoblotting of the 2D gels with anti-SAHH and anti-ADK antibodies (Fig. 4B). Tandem mass spectrometry (MS/MS) analysis of the protein spots revealed the presence of both SAHH1 and SAHH2 isoforms in two different oligomeric protein complexes, which migrated at different positions on CN-PAGE (Fig. 4A). It is worth noting that the SAHH-containing spot originating from the lower M_r oligomer also contained calreticulin-1, an endoplasmic reticulum-resident lectin chaperone (Fig. 4A; Table II). Notably, however, immunoblotting with anti-SAHH antibody confirmed both the location and the up-regulation of SAHH in *pp2a-b′γ* as compared with wild-type plants (Fig. 4B).

In the Met-salvage pathway, SAHH hydrolyzes *S*-adenosyl-L-homocysteine, the reaction product of

Table II. *Summary of proteins and phosphopeptides identified from soluble leaf extracts by 2D CN-PAGE and MS/MS analysis*

Spot Identifier and Change in *pp2a-b′γ* [a]	Full Name	Gene	Score/Coverage	Phosphopeptides[b]
Defense and stress				
TGG1 ↑	Thioglucoside glucohydrolase 1	AT5G26000	2,732/39%	R.GYALG(p)TDAPGR.C K.GFIFGVAS(p)SAYQVEGGR.G R.EYVGDRLPEF(p)SETEAALVK.G K.EKYE(p)TNPALYGELAK.G
CA1 ↑	Carbonic anhydrase1	AT3G01500	1,224/27%	
AtGSTF2 ↑	Glutathione *S*-transferase F2	AT4G02520	1,028/58%	
CSD2 ↑	Copper/zinc superoxide dismutase	AT2G28190	229/32%	
Amino acid metabolism and Met cycle				
OLD3 ↑	Onset of leaf death 3/*O*-acetyl-Ser(thiol)lyase	AT4G14880	688/40%	
SAHH1 ↑	*S*-Adenosyl-L-homocysteine hydrolase 1	AT4G13940	1,375/39%	R.LVGV(p)SEETTTGVK.R R.I(p)TIKPQTDR.W[c]
SAHH2 ↑	*S*-Adenosyl-L-homocysteine hydrolase 2	AT3G23810	265/18%	
ADK1 ↑	Adenosine kinase 1	AT3G09820	484/39%	
ADK2 ↑	Adenosine kinase 2	AT5G03300	482/35%	
GS2 ↓	Gln synthetase 2	AT5G35630	694/24%	R.(p)TIEKPVEDPSELPK.W
GS1.2	Gln synthetase 1;2	AT1G66200	143/10%	
AtGLN1;1 ↑	Gln synthetase 1;1	AT5G37600	262/24%	
AGT1	Ala-glyoxylate aminotransferase	AT2G13360	499/25%	K.(p)TLLEDVKK.I K.L(p)SQDENHTIK.A
Carbon metabolism				
TKL ↑	Transketolase	AT3G60750	902/30%	K.(p)TVTDKPTLIK.V K.(p)SIITGELPAGWEK.A K.AN(p)SYSVHGAALGEK.E R.HTPEGA(p)TLESDWSAK.F
FBA	Fru bisphosphate aldolase	AT4G38970	582/30%	K.Y(p)TGEGESEEAK.E R.A(p)TPEQVAAYTLK.L K.DRA(p)TPEQVAAYTLK.L K.RLDSIGLEN(p)TEANR.Q
MDH	Malate dehydrogenase	AT1G04410	774	
FBP	Fru-1,6-bisphosphatase	AT1G43670	681/46%	
PRK ↑	Phosphoribulokinase	AT1G32060	1,731/28%	K.FYGEV(p)TQQMLK.H
IDH	Cytosolic $NADP^+$-dependent isocitrate dehydrogenase	AT1G65930	711/17%	
Other				
CA2	Carbonic anhydrase 2	AT5G14740	642/50%	
CRT1	Calreticulin 1	AT1G56340	587/33%	
Cpn60α ↑	Chaperonin-60α	AT2G28000	785/31%	

[a]The spot identifications are as presented in Figure 4. Protein spots showing higher or lower intensity as compared with the wild type are indicated by arrows. [b]For identification of phosphopeptides, Mascot analysis of MS/MS spectra was conducted by restricting searches for the Arabidopsis database and allowing phosphorylation of Thr and Ser residues as possible modifications. [c]This peptide was detected with a score below the statistical limit for reliable identification.

transmethylation reactions, to adenosine and homocysteine. Adenosine in turn becomes phosphorylated by ADK to avoid end product-mediated inhibition of SAHH (Moffatt and Weretilnyk, 2001). ADK isoforms were found to comigrate with SAHH in the lower M_r oligomer on CN-PAGE (Figs. 4, A and B).

For the identification of phosphoproteins, the acquired MS/MS spectra were analyzed by allowing phosphorylation of Ser and Thr residues as possible modifications in Mascot searches against the Arabidopsis database. This approach revealed the presence of phosphopeptides in SAHH1, TGG1, FBA, TKL, phosphoribulokinase, Gln synthase 2 (GS2), and Ala glyoxylate aminotransferase (AGT1; Table II).

To gain insights into possible differences in the pattern of protein phosphorylation between *pp2a-b′γ* and wild-type plants, 2D CN-PAGE gels were subjected to immunoblotting with phospho-Thr-specific antibody (Fig. 4C). The immunoblot was overlaid with a SYPRO-stained 2D gel, and the detected phosphoproteins were identified as SAHH1, FBA, GS2, and AGT1 based on the relative locations of Rubisco subunits on the gel and on the presence of phosphopeptides in the MS/MS spectra, as presented in Table II. The phosphorylation of Rubisco large subunit on Thr residues has been demonstrated earlier (Lohrig et al., 2009). As shown in Figure 4C, the immunoreaction with phospho-SAHH1 was stronger in *pp2a-b′γ* than in wild-type plants, whereas all other

phosphoproteins showed similar or reduced levels in *pp2a-b′γ* as compared with wild-type plants. Some of the detected phosphoproteins remained unidentified, as they were not visible on SYPRO-stained or silver-stained gels.

Finally, the up-regulation of CSD2 in *pp2a-b′γ* (Fig. 4B) prompted us to utilize one-dimensional SDS-PAGE to explore the levels of chloroplastic and cytoplasmic antioxidant enzymes in *pp2a-b′γ* and wild-type leaves. The steady-state levels of chloroplastic and cytoplasmic ascorbate peroxidases as well as the chloroplast 2-Cys peroxiredoxin and peroxiredoxin E showed no consistent differences between *pp2a-b′γ* and wild-type plants (Fig. 4D). However, the steady-state level of peroxiredoxin Q was clearly reduced, and the level of chloroplastic glutathione peroxidase 7 was also slightly lower in *pp2a-b′γ* plants (Fig. 4D). Altogether, the proteome of *pp2a-b′γ* seems to respond to defense- and ROS-related pathway changes in leaf tissue.

Light Sensitivity of Wild-Type and *pp2a-b′γ* Leaves

Next, we explored whether the apparent degeneration of cells in *pp2a-b′γ* leaves (Fig. 2) and the differential adjustments in levels of antioxidant enzymes (Fig. 4) were accompanied by light-dependent imbalances in ROS metabolism. Staining with nitroblue tetrazolium showed distinct accumulation of O_2^- in the oldest leaves of *pp2a-b′γ* plants under normal growth light conditions, whereas in wild-type leaves the accumulation of O_2^- was remote (Fig. 5A). O_2^- is rapidly dismutated to H_2O_2 (Foyer and Noctor, 2009). Moreover, ROS production is enhanced under high light, a phenomenon that promotes cell death in various lesion-mimic mutants (Lorrain et al., 2003). To determine the extent of H_2O_2 accumulation upon sudden changes in light conditions in *pp2a-b′γ* and wild-type plants, the rosettes were floated on 0.1% DAB and illuminated under low light, growth light, or high light (with 20, 130 or 1,000 μmol photons m^{-2} s^{-1}, respectively) for 2 h. Under low-light conditions, wild-type plants showed hardly any accumulation of H_2O_2 (Fig. 5A), but with increasing light intensities, the accumulation of H_2O_2 was observed as brown precipitate on the leaves (Fig. 5A). In the oldest leaves of *pp2a-b′γ* plants, distinct accumulation of H_2O_2 was detected already under low-light conditions, and DAB staining was further enhanced when the plants were illuminated under growth light (Fig. 5A). Microscopic examination showed intense DAB staining of H_2O_2 particularly in chloroplasts of distinct mesophyll cells in *pp2a-b′γ* leaves (Fig. 5B). Under high irradiance, however, the difference in DAB staining between *pp2a-b′γ* and the wild type started to level off (Fig. 5A). Accordingly, a gradual PSII photoinhibition of similar extent (measured as F_v/F_m [see "Materials and Methods"] after a 30-min dark incubation) was measured for both the wild type and *pp2a-b′γ* upon exposure of plants to 1,000 μmol of photons $m^{-2}s^{-1}$ at 20°C for 4 h (Fig. 5C). Thus, PP2A-B′γ does not contribute to the vulnerability of plants upon sudden onset of high irradiance.

Defense Responses in *pp2a-b′γ* Plants

Next, it was tested whether the adjustments in defense-associated components (Table II; Fig. 4) altered the *pp2a-b′γ* mutant's response toward different types of plant pathogens. Virulent *Pseudomonas syringae* pv *tomato* DC3000 was gently syringe infiltrated at 10^8 colony-forming units mL^{-1} into the leaves of *pp2a-b′γ* and wild-type plants. During the first 2 d post infection, no significant differences in bacterial growth on the leaves of *pp2a-b′γ* and wild-type plants could be observed (Fig. 6A). Five days post infection, however, 8-fold higher bacterial titers were counted on the leaves of wild-type plants than on the leaves of *pp2a-b′γ* plants (Fig. 6A).

To assess the ability of *pp2a-b′γ* plants to resist a necrotrophic fungus, lesion formation upon infection by *Botrytis cinerea* was compared with that in the wild type. Two days post infection, visually observable macerated lesions appeared on wild-type leaves (Fig. 6B). By contrast, *pp2a-b′γ* mutant plants clearly developed less necrotic symptoms (Fig. 6B). Thus, in accordance with the constitutive expression of defense-related genes (Supplemental Table S1), *pp2a-b′γ* mutant plants show increased resistance to both a hemibiotrophic and a necrotrophic pathogen.

Global DNA Methylation in *pp2a-b′γ* Plants

Bacterial infections have been shown to induce changes in the pattern of DNA methylation in plants (Pavet et al., 2006). Furthermore, SAHH1, which showed elevated levels in *pp2a-b′γ* leaves (Fig. 4), has also been identified as HOMOLOGY-DEPENDENT GENE SILENCING1 (HOG1) and proposed to mediate epigenetic regulation through the maintenance of cellular transmethylation capacity (Rocha et al., 2005). Thus, we explored whether the knockdown of *PP2A-B′γ* modulates the level of DNA methylation in leaves. To this end, DNA was digested with methylation-sensitive restriction enzymes, which cut unmethylated CCGG sites on DNA, and the global level of DNA methylation was explored by Southern blotting using the repetitive unit of 5S rDNA as a probe. As shown in Figure 7, an increased appearance of restriction products indicative of slight hypomethylation was observed in DNA isolated from *pp2a-b′γ* leaves. Similar accumulation of DNA restriction products (Fig. 7) was observed with DNA isolated from the yellowing plants overexpressing *PP2A-B′γ-YFP* (Fig. 1A). In contrast, the level of DNA methylation in the complemented *pp2a-b′γ* line expressing *PP2A-B′γ* coding sequence under the 35S promoter was comparable to that of wild-type plants (Figs. 1 and 7).

DISCUSSION

Regulatory Subunit B′γ of PP2A Prevents Inappropriate Defense Reactions

A fundamental property of type 2A protein phosphatases is that their specificity is conferred by variable

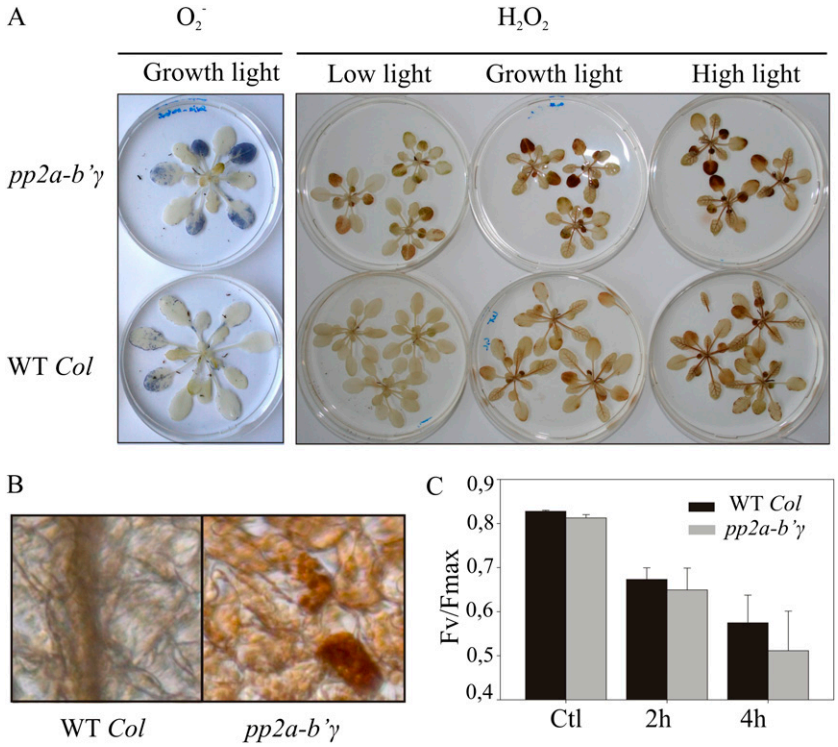

Figure 5. ROS metabolism in wild-type (WT Col) and *pp2a-b′γ* mutant plants. A, Accumulation of O_2^- and H_2O_2. O_2^- was visualized as a blue precipitate after floating of rosettes on nitroblue tetrazolium for 2 h under normal growth light conditions. For visualization of H_2O_2, rosettes were floated on 0.1% DAB under low light, under normal growth light conditions, and under high light (20, 130, and 800 μmol photons m^{-2} s^{-1}, respectively). The accumulation of H_2O_2 is visualized as a brown precipitate on the leaves. B, Stereomicrographs demonstrating the cellular location of H_2O_2 in wild-type and *pp2a-b′γ* leaves. C, Photoinhibition of PSII in 4-week-old plants exposed to 1,300 μmol photons m^{-2} s^{-1} for 4 h. The photochemical efficiency of PSII was measured as F_v/F_m after a 30-min dark incubation. The values are means ± SD of three independent experiments.

regulatory B subunits, which direct the trimeric PP2A holoenzyme to the accurate target proteins. We have identified a regulatory B′γ subunit of PP2A that contributes to developmental regulation and stress tolerance in Arabidopsis. In plants, the spatiotemporal availability of individual A, B, and catalytic subunits represents an important means of regulation at the level of PP2A complex formation. We found that *PP2A-B′γ* is expressed in patches in the peripheral parts of rosette leaves (Fig. 1). Knockdown of *PP2A-B′γ* is sufficient to induce several hallmarks of defense reactions, including constitutive expression of disease resistance genes, accumulation of ROS, and premature yellowing in *pp2a-b′γ* leaves (Figs. 1–3; Table II). This reveals a specific and central role for the PP2A-B′γ subunit as a negative regulator that prevents premature senescence and unnecessary defense responses in Arabidopsis.

Activation of defense mechanisms upon infection is known to involve phosphorelay cascades, of which a number of protein kinases with crucial signaling roles have been identified (Xing et al., 2002). In many cases, the target phosphoproteins and the counteracting protein phosphatases have remained unidentified, but a number of phosphoproteins, including receptor-like kinases and protein phosphatases with evident signaling functions in different phases of infection, have been identified by proteomic approaches (Jones et al., 2006; Benschop et al., 2007; Nühse et al., 2007). For example, recognition of bacterial flagellin by receptor-like kinase FLS2 leads to activation of the mitogen-activated protein kinase pathway, which is one of the key phosphorelay cascades that modulate the activity of defense-related genes in plants (Tena et al., 2001; Qiu et al., 2008). A PP2C-type protein phosphatase, AP2C1, modulates innate immunity through negative regulation of MPK4 and MPK6 (Schweighofer et al., 2007). Notably, PP2Cs are monomeric enzymes, which makes the analysis of their target processes rather straightforward. PP2A as a heterotrimer is structurally more complex, and the large number of isoforms for each subunit provide extensive variability for the composition of the PP2A holoenzyme. Whereas the methodology to pull down enzymatically active PP2A complexes from Arabidopsis already exists (Tang et al., 2011), reconstitution of PP2A heterotrimers with the desired composition of catalytic C and regulatory A and B subunits has not been reported thus far. Therefore, cognate targets recognized by specific regulatory B subunits of heterotrimeric PP2A-type protein phosphatases in plant defense responses have so far remained unidentified. Nevertheless, the presence of catalytic PP2A subunits is known to be required for the negative regulation of defense responses in tobacco (He et al., 2004). We demonstrate here for Arabidopsis that the regulatory B′γ subunit mediates negative control of PP2A in defense signaling, most likely by determining the specificity of interaction between PP2A and the target phosphoprotein(s).

PP2A-B′γ-Dependent Signals Specifically Modulate Components of the Cellular Antioxidant Network

Resistance against invading pathogens necessitates tight cross-communication between different signal-

ing pathways in plants. Chloroplasts are highly responsive to external cues and carry out versatile functions in the regulation of defense reactions upon infection. It has become well known that light-induced ROS production through photosynthetic electron transport promotes the rapid onset of cell death in response to biotrophic pathogens (Bechtold et al., 2008). Accordingly, a number of lesion-mimic mutants with enhanced hypersensitive reaction-like cell death under high irradiance levels have been identified (Lorrain et al., 2003). For example, *lesion-simulating disease1* shows a runaway cell-death phenotype because it fails to transmit chloroplast redox signals to up-regulate antioxidant genes under photooxidative conditions (Mateo et al., 2004). In contrast, *pp2a-b′γ* mutants are not prone to high-light-induced damage in chloroplasts and display increased resistance to both biotrophic and necrotrophic pathogens (Figs. 3, 5, and 6).

In connection with the importance of chloroplast-derived ROS as key signaling molecules, the function of antioxidant enzymes and ROS scavenging in the fine-tuning of defense reactions has also been recognized. In *pp2a-b′γ* leaves, the constitutive defense

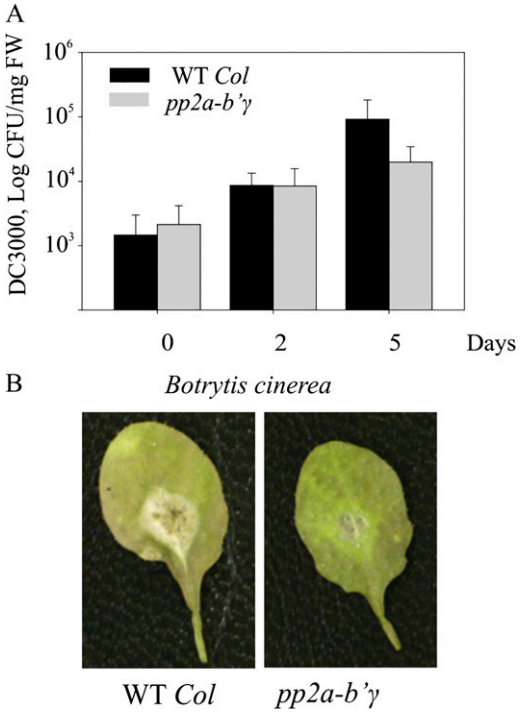

Figure 6. Defense responses in *pp2a-b′γ* mutant plants. A, Suppressed growth of *P. syringae* pv *tomato* DC3000 in *pp2a-b′γ*. Bacterial growth was followed at 0, 2, and 5 d after gentle syringe infection with a bacterial suspension corresponding to 10^8 colony-forming units (CFU) in 10 mM $MgCl_2$. The data are expressed as mean CFU mg^{-1} fresh weight (FW) ± SD ($n = 4$ for days 0 and 2, $n = 5$ for day 5). B, Reduced lesion formation in *pp2a-b′γ* leaves upon infection by *B. cinerea*. Lesion formation in wild-type (WT Col) and *pp2a-b′γ* plants was compared 2 d post infection.

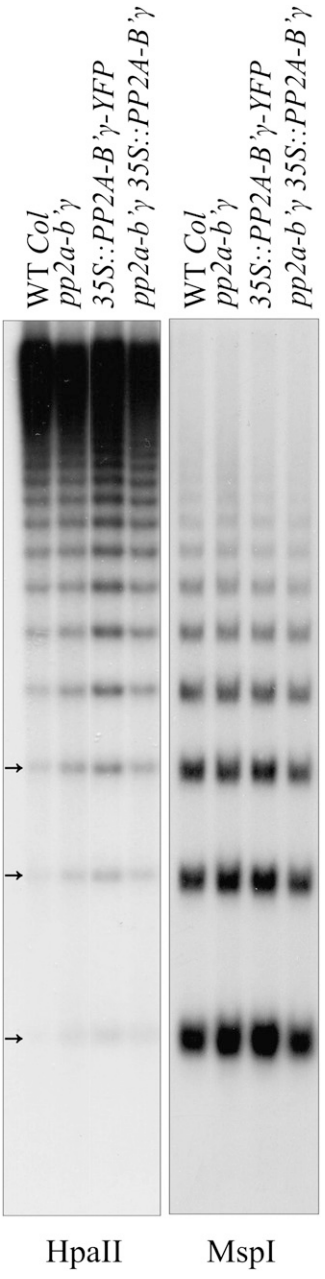

Figure 7. Southern blots demonstrating the global status of DNA methylation in wild-type (WT Col) and *pp2a-b′γ* plants. Genomic DNA was isolated from 5-week-old wild-type plants, the *pp2a-b′γ* mutant, a line overexpressing *PP2A-B′γ-YFP* in the wild-type background, and *pp2a-b′γ* complemented by 35S-driven expression of the *PP2A-B′γ* gene. One microgram of DNA was digested with methylation-sensitive restriction enzymes (*Hpa*II and *Msp*I) and visualized using a probe against the repetitive unit of Arabidopsis 5S rDNA. *Hpa*II does not cut if the first or second cytosine of the restriction site is methylated ($^mC^mCGG$), whereas *Msp*I is sensitive to methylation of the second cytosine (C^mCGG). Thus, increased detection of restriction products (denoted by arrows) on the Southern blot indicates hypomethylation of DNA.

responses and elevated ROS levels associate with increased levels of the chloroplast copper/zinc superoxide dismutase CSD2 (Fig. 4B). This is paralleled by an elevated level of ACO (Fig. 4), which, in addition to its classical function in the mitochondrial citric acid cycle, has also been proposed to regulate the function of CSD2 via binding into the 5′ untranslated region of *CSD2* mRNA in the cytoplasm (Moeder et al., 2007). Intriguingly, *Nicotiana benthamiana* plants with reduced ACO levels displayed increased resistance against MV-induced photooxidative stress, which further supports a role for ACO in the antioxidant network in plants (Moeder et al., 2007). Moreover, ACO seems to mediate complex interactions in plant defense responses against biotrophic pathogens by promoting cell death at early phases of infection but restricting spread of the lesions at later times of infection (Moeder et al., 2007). The mechanism of action, however, remains unresolved.

In contrast to the up-regulation of CSD2, the constitutive defense responses in *pp2a-b′γ* involve specific down-regulation of the H_2O_2-scavenging enzymes glutathione peroxidase 7 and peroxiredoxin Q in chloroplasts (Fig. 4D). This is in line with a recent report demonstrating that Arabidopsis plants lacking chloroplast glutathione peroxidases are more vulnerable to photooxidative stress than the wild type but resistant against infection by *Pseudomonas* strains (Chang et al., 2009). Another study indicated a role for peroxiredoxin Q in mediating responses against *Botrytis*, a necrotrophic fungus (Kiba et al., 2005). These data collectively suggest that PP2A-B′γ-dependent defense signaling modifies the levels of CSD2, ACO, glutathione peroxidase, and peroxiredoxin Q, which, in turn, are specifically involved in the fine-tuning of defense reactions according to internal and external cues in plant cells.

PP2A-B′γ- and CPR5-Dependent Signaling Cascades Regulate Cell Death under Low Irradiance Levels

A recent proteomic analysis of *cpr5* suggests that CPR5 operates in the maintenance of cellular redox balance and the regulation of senescence in Arabidopsis leaves (Jing et al., 2008). In line with this conclusion, two mutants originally identified as *onset of leaf death1* and *hypersenescence1* were found to harbor a mutation in *CPR5* (Yoshida et al., 2002; Jing et al., 2008). Since *pp2a-b′γ* plants also exhibit senescence-like characteristics, it appears that the activity of B′γ-containing PP2A complexes is needed to prevent premature leaf senescence as well. The *PP2A-B′γ* promoter is active in patches in the peripheral parts of rosette leaves, a pattern that highly resembles the onset of yellowing in early phases of senescence (Fig. 1). Furthermore, visually presymptomatic *pp2a-b′γ* leaves show degeneration of chloroplasts (Fig. 2), one of the earliest symptoms of senescence, long before the yellowing spots appear on the leaf blades of aging *pp2a-b′γ* plants (Fig. 1). In particular, the spongy mesophyll tissue of *pp2a-b′γ* leaves harbors shrinking cells with almost completely disintegrated organelles (Fig. 2). On the other hand, *pp2a-b′γ* mutants also exhibit enhanced expression of cell death antagonists, presumably to limit the speed of lesion formation (Supplemental Table S2). Indeed, senescence is a tightly regulated developmental program, in which cell death starts at local patches of early-dying cells and then slowly propagates to neighboring cells in a strictly controlled manner (Lim et al., 2007). Senescence is also tightly connected with defense responses and can be enhanced by pathogen infection (Butt et al., 1998; Quirino et al., 1999). This might be a means for plants to decrease nutrient availability and thereby limit pathogen growth. Notably, enhanced senescence also represents a mechanism for cell death induction under low irradiance levels.

Comparison of *pp2a-b′γ*, *cpr5*, and the *pp2a-b′γ cpr5* double mutant revealed that accumulation of H_2O_2 and sensitivity to photooxidative stress in *pp2a-b′γ* require the presence of functional CPR5 (Fig. 3). Even though the *pp2a-b′γ cpr5* double mutant shows additive suppression of growth and malformation of trichomes, it resembles *cpr5* with respect to the accumulation of defense hormones and tolerance against photooxidative stress (Fig. 3). Thus, *CPR5* is epistatic to *PP2A-B′γ* with respect to defense signaling. These findings demonstrate that PP2A-B′γ- and CPR5-dependent pathways are functionally connected and prevent in concert the unnecessary defense reactions under low irradiance levels in Arabidopsis.

PP2A-B′γ-Dependent Adjustments in Methyl Recycling May Contribute to Epigenetic Regulation of Defense Gene Expression

In contrast to the majority of lesion-mimic mutants identified to date, *pp2a-b′γ* as well as *cpr5* and the *pp2a-b′γ cpr5* double mutant show premature yellowing under moderate light intensity, whereas high light does not retard growth (Fig. 3B). A similar observation has been made for another lesion-mimic mutant, *defense no death1* (*dnd1*; Mateo et al., 2006). In *cpr5*, the mutation lies in a gene coding for a membrane protein of unknown function, whereas *dnd1* is deficient in cyclic nucleotide-gated cation channel 2 (Clough et al., 2000; Ali et al., 2007). The dwarfish low-light phenotypes of *cpr5* and *dnd1* were discussed in terms of an enhanced accumulation of foliar SA, but no functional connection between CPR5 and DND1 has been reported (Mateo et al., 2006). Notably, although both *cpr5* and *pp2a-b′γ* show constitutive up-regulation of both SA and JA marker genes, *pp2a-b′γ* demonstrated no increase in the levels of either SA or JA (Fig. 3D). These results suggest that in defense signaling, PP2A-B′γ operates downstream of hormonal responses.

Increasing evidence suggests crucial roles for epigenetic mechanisms in plant immunity, as reviewed by Alvarez et al. (2010). Transcriptional activation involves the unfolding of chromatin structure through combined effects of changes in the level of DNA and histone

methylation, binding of histone variants, and activity of chromatin-remodeling complexes. Indeed, hypomethylation of DNA may promote the expression of defense-related genes by mediating decondensation of the chromatin structure (Pavet et al., 2006). In Arabidopsis, basal repression of the SA-dependent defense pathway in noninfected plants involves chromatin remodeling through SUPPRESSOR OF NPR1 INDUCED1 (SNI1) as well as the SUC NONFERMENTING2 family members PHOTOPERIOD-INDEPENDENT EARLY FLOWERING1 (PIE1) and the functionally less-well-characterized BRAHMA101 (BRM101; Bezhani et al., 2007; Deal et al., 2007; Durrant et al., 2007). Analysis of gene expression profiles revealed 11 common SA-responsive genes constitutively up-regulated in *sni1*, *pie1*, and *brm101* mutants (Alvarez et al., 2010). Transcript levels for these genes are also constitutively higher in *pp2a-b′γ* as compared with wild-type plants (Supplemental Table S1), even though no differences in the levels of SA/JA are observed in the mutant leaves (Fig. 3D). The level of DNA methylation, however, is slightly decreased, and the increased levels of SAHH1/HOG1 and ADK suggest an altered balance of cellular methylation reactions in *pp2a-b′γ* leaves (Figs. 4 and 7). These findings suggest that PP2A-B′γ-dependent signaling events contribute to the regulation of defense reactions at the DNA level.

Besides SAHH1/HOG1 and ADK of the Met-salvage pathway (Moffatt and Weretilnyk, 2001), *pp2a-b′γ* leaves contain increased levels of the Cys synthase OLD3, which also contributes to the biosynthesis of glutathione and Met (Fig. 4; Shirzadian-Khorramabad et al., 2010). Pathways involved in the recycling and de novo synthesis of Met are, in turn, tightly connected with the biosynthesis of aliphatic glucosinolates, which release toxic compounds through myrosinase activity in response to herbivore or microbial attack (Hirai et al., 2007; Fan et al., 2011). Intriguingly, the constitutive defense response in *pp2a-b′γ* leaves also involves an increased level of myrosinases, and their function may be controlled through reversible phosphorylation (Fig. 4; Table II). Indeed, glucosinolates, Cys, and Met constitute key sulfur-containing molecules, whose levels are tightly interregulated through complex feedback loops in plant cells (Hoefgen and Nikiforova, 2008). It is also worth noting that *S*-adenosyl Met serves as a precursor for the biosynthesis of ethylene, thus forming another crucial connection between Met homeostasis and the regulation of defense reactions and senescence in plants (Amir, 2010). Taken together, PP2A-B′γ may influence the levels of sulfur-containing compounds and DNA methylation through the regulation of Met-related metabolic reactions in leaves.

CONCLUSION

We have demonstrated that a specific B′γ subunit of PP2A is functionally connected with CPR5 and mediates the negative regulation of defense reactions and senescence under low irradiances in Arabidopsis. Furthermore, the constitutively higher levels of defense-related transcripts, together with hypomethylation of DNA and increased levels of the Met-salvage pathway components SAHH and ADK in *pp2a-b′γ* leaves, suggest that PP2A-B′γ may contribute to the epigenetic regulation of defense gene expression. Current attempts to identify the PP2A-B′γ-interacting proteins and the target phosphoproteins will finally specify the mechanistic function of PP2A-B′γ in the regulation of cellular processes in Arabidopsis.

MATERIALS AND METHODS

Materials and Growth Conditions

Arabidopsis (*Arabidopsis thaliana*) ecotype Columbia wild type and the mutants were grown under control conditions of 130 μmol photons m^{-2} s^{-1}/22°C (growth light) or under 800 μmol photons m^{-2} s^{-1}/24°C (high light) with 50% humidity and an 8-h light period. Homozygote *pp2a-b′γ* (SALK_039172 for At4g15415) and *pp2a-b′ζ* (SALK_107944C for At3g21650) mutant lines were identified from the SALK Institute's collection by PCR analysis according to the institute's protocols (Alonso et al., 2003). Insertion mutant information was obtained from the SIGnAL Web site at http://signal.salk.edu.

The *cpr5* mutant (N3770; At5g64930) was obtained through the Nottingham Arabidopsis Stock Centre (http://nasc.nott.ac.uk). A *pp2a-b′γ cpr5* double mutant was constructed by crossing the *pp2a-b′γ* and *cpr5* single mutants. Mutants homozygous for *cpr5* were first selected from the F2 generation based on the absence of trichomes on leaves (Kirik et al., 2001), and individuals homozygous for *pp2a-b′γ* were further identified by PCR using the same set of primers that were used to screen for the single *pp2a-b′γ* mutants.

Construction of Transgenic Lines

For genetic complementation of the *pp2a-b′γ* mutation, the protein-coding sequence of the *PP2A-B′γ* gene (S69317; Yamada et al., 2003) was cloned into the binary plant expression vector pGREENII0029 under the control of the 35S cauliflower mosaic virus promoter. For spatial analysis of *PP2A-B′γ* promoter activity, wild-type Arabidopsis plants were transformed with a *promoter*::*uidA* fusion construct containing a 2.8-kb region of genomic DNA upstream of the translational start codon of the *PP2A-B′γ* coding sequence. After sequencing of the resulting constructs, *pp2a-b′γ* plants were transformed by floral dipping. GUS staining of expanded leaves expressing the *promoter*::*uidA* fusion was performed according to Weigel and Glazebrook (2002) and imaged with a Zeiss Lumar V12 stereomicroscope (http://www.zeiss.com).

For subcellular localization, the *PP2A-B′γ* coding sequence (S69317; Yamada et al., 2003) without the translational stop codon was fused in frame with YFP in the pGREENII0029-based vector under the control of the 35S promoter. The vector was introduced into Arabidopsis protoplasts isolated from 4- to 5-week-old plants according to previously established methods (Negrutiu et al., 1987; Damm et al., 1989).

Electron Microscopy

Leaves of 4-week-old plants, not showing visual symptoms of yellowing, were fixed with 2.5% glutaraldehyde in 75 mM sodium cacodylate buffer, pH 7.2, under mild vacuum for 30 min and postfixed with 1% osmium tetraoxide in the same buffer. The tissues were then dehydrated in a graded series of acetone and stained with 1% uranyl acetate in 20% acetone. The samples were embedded in Spurr's resin, polymerized at 60°C, poststained with lead citrate, and finally examined with an electron microscope (10-Sx; JEOL). Degrading chloroplasts that showed loosening of the thylakoid membrane and roundish or irregular morphology were calculated from eight different images for each cell type.

Laser Scanning Confocal Microscopy

Fluorescence from YFP was imaged with a confocal laser scanning microscope (Zeiss LSM510 META; http://www.zeiss.com) with excitation at 514

nm and detection at 535 to 590 nm. Chlorophyll fluorescence was excited at 543 nm and detected with a 650-nm passing emission filter. Trichomes were imaged after a 5-min staining of cell walls with 10 μg mL^{-1} Hoechst 33258 (Invitrogen; www.invitrogen.com). Detection was performed at 420 to 480 nm after excitation at 405 nm. Cell death was examined after gently infiltrating the leaves with 0.5 mg mL^{-1} propidium iodide. Detection of intracellular fluorescence indicative of membrane disruption was performed at 590 to 650 nm after excitation at 488 nm. For all applications, maximal projections of the sequential confocal images were created with Zeiss LSM Image Browser version 3.5.0.376 (http://www.zeiss.com).

Analysis of Gene Expression

Four-week-old rosettes of wild-type and *pp2a-b′γ* mutant plants grown under normal growth conditions (130 μmol photons m^{-2} s^{-1}) or under high light (800 μmol photons m^{-2} s^{-1}) were collected 2 h after the onset of the light period. Changes in gene expression were explored with spotted Arabidopsis 24k oligonucleotide arrays (MWG Biotech; http://www.mwg-biotech.com; ArrayExpress database accession no. A-ATMX-2; http://www.ebi.ac.uk/arrayexpress) according to Piippo et al. (2006) from three biological replicates using GeneSpring 7.2. Gene annotation was derived from the Arabidopsis Information Resource (http://www.arabidopsis.org).

For quantitative real-time PCR, total RNA was extracted as described (Piippo et al., 2006), followed by DNase treatment using the TURBO DNA-Free Kit (Ambion; http://www.ambion.com). Subsequently, cDNA synthesis was carried out with the ISCRIPT cDNA Synthesis Kit (Bio-Rad Laboratories; http://www.bio-rad.com). Real-time PCR was performed using iQ SYBR GREEN SUPERMIX (Bio-Rad Laboratories). *PP2A-B′γ* cDNA was specifically amplified with the primers FOR (5′-TCAACGAGCTCTAACAGAACCAATCAAGTC-3′) and REV (5′-AACAGCCACTTTCGCAATC-3′).

Analysis of ROS Metabolism and Photosynthetic Properties

The sensitivity of plants to MV-induced photooxidative stress was explored with 50 μM MV as described by Kangasjärvi et al. (2008). For detection of O_2^-, detached rosettes were floated on 0.1% nitroblue tetrazolium (Sigma-Aldrich; http://www.sigmaaldrich.com) with 10 mM NaN_3 in 10 mM phosphate buffer, pH 7.8, overnight in darkness, then illuminated under normal growth conditions for 2 h, and finally cleared in 96% (v/v) ethanol. Accumulation of H_2O_2 in the leaves was detected by using DAB (Sigma-Aldrich) as a substrate (Thordal-Christensen et al., 1997) with the modifications described (Kangasjärvi et al., 2008) and finally photographed with a Zeiss Lumar V12 stereomicroscope (http://www.zeiss.com).

Photosynthetic activity was measured under normal growth light (130 μmol photons m^{-2} s^{-1}/22°C) with the CIRAS-1 combined infrared gas analysis system (PP Systems) equipped with an Arabidopsis pot chamber (PP Systems). The photoinhibition state of PSII in intact leaves was recorded as the ratio of variable to maximal fluorescence (F_v/F_m, where F_v is the difference between maximal fluorescence [F_m] and initial fluorescence), measured with a Hansatech PEA fluorometer after a 30-min dark incubation. Blue native gel electrophoresis of thylakoid protein complexes was performed as described by Lepistö et al. (2009).

Isolation of Total and Soluble Leaf Extracts, 2D CN-PAGE, Mass Spectrometry, and Immunoblotting

Extraction of total foliar extracts and total soluble leaf extracts was performed in the presence of protease (Complete-Mini; Roche) and phosphatase (PhosSTOP; Roche) inhibitors using the methods described by Kangasjärvi et al. (2008). Total soluble leaf extracts corresponding to 80 and 10 μg of proteins were used for analysis by mass spectrometry and immunoblotting, respectively. Soluble oligomeric protein complexes were separated by CN-PAGE followed by SDS-PAGE in the second dimension according to Peltier et al. (2006) with the modifications for buffers described (Rokka et al., 2005), except that only 0.05% deoxycholate was used as a detergent on CN gels. After imaging the gels with SYPRO Ruby (Invitrogen), mass spectrometry was performed as described by Peltier et al. (2006) using a liquid chromatography-electrospray ionization-MS/MS system (QTOF Elite; AB Sciex). MS/MS spectra were analyzed with an in-house installation of Mascot (www.matrixscience.com), with searches restricted to the Swissprot Arabidopsis database, allowing Met oxidation, Cys carboamidomethylation, and Ser/Thr phosphorylation as possible modifications.

Immunoblotting with anti-phospho-Thr and protein-specific antibodies was performed as described (Kangasjärvi et al., 2008). For detection of phosphoproteins, total soluble leaf extracts corresponding to 80 μg of protein were separated by 2D CN-PAGE, transferred onto a polyvinylidene difluoride membrane (Immobilon-P; Millipore), blocked with 5% (w/v) specific fat-free bovine serum albumin (Sigma), and probed with polyclonal anti-phospho-Thr antibody (P-Thr-Polyclonal; New England Biolabs) diluted 1:1,000 in 5% (w/v) fat-free bovine serum albumin, 1× Tris-buffered saline, and 0.1% Tween 20. According to the manufacturer's instructions, the P-Thr-Polyclonal antibody binds phospho-Thr in a manner largely independent of the surrounding amino acid sequence. Other antibodies were obtained from Agrisera (http://www.agrisera.se/) or were kindly provided by Prof. K.-J. Dietz (2-Cys peroxiredoxin, peroxiredoxin IIE, and peroxiredoxin Q) and by Prof. B. Moffat (SAHH and ADK1). The total level of 2-Cys peroxiredoxin was explored according to König et al. (2003). The antibody against PP2A-B′γ was raised against the peptides NDPSKNLREKEIKRC and PAMERNTRGHWNQAC (www.antiprot.com) and tested against a cell lysate of *Escherichia coli* transformed with a pET28 (www.invitrogen.com) containing a C-terminal 6xHIS-tagged *PP2A-B′γ* coding sequence.

Analysis of DNA Methylation

Analysis of DNA methylation was performed as described (Pavet et al., 2006) with slight modifications. In brief, DNA was extracted with phenol/chloroform, and 1 to 3 μg of DNA was digested with methylation-sensitive enzymes (*Hpa*II or *Msp*I; New England Biolabs), subjected to electrophoresis on a 1.2% agarose gel, and blotted onto a Hybond N$^+$ membrane. The highly repeated tandem unit of 5S rDNA (Campell et al., 1992) was PCR amplified using the primers 5′-TCGGGCATTTTCGTGATTTGGGC-3′ (forward) and 5′-AAGTTGTCCTGCTTCTTTCGTCGG-3′ (reverse), purified with NucleoSpin Extract II (Macherey-Nagel), labeled with [α-^{32}P]dCTP using random hexamer priming (Prime-a-Gene labeling system; Promega), and finally used for hybridization of the membrane at 65°C overnight.

Analysis of Hormone Levels and Defense Responses

Plant hormones were analyzed using a modified vapor-phase extraction method (Schmelz et al., 2003) as described (Lepistö et al., 2009) without the final silylation step for the analysis of JA. As internal standards, 50 ng of [^{13}C] SA and 50 ng of dihydrojasmonic acid were added to the extraction buffer.

For infection of plants, *Pseudomonas syringae* pv *tomato* DC3000 was grown in NYG medium (0.5% tryptopeptone, 0.3% yeast extract, and 2% glycerol) at 28°C overnight. Thereafter, 4-week-old plants were infected gently using a needleless syringe on the lower side of the leaf using 10^8 colony-forming units mL^{-1} and 10 mM $MgCl_2$. For each time point, eight leaves corresponding to 1.2 mg fresh weight were pooled and ground in 10 mM $MgCl_2$, and bacterial count mg^{-1} fresh weight was assessed as described earlier (Yu et al., 1998).

Leaves of Arabidopsis were inoculated with 10-μL conidial suspensions (2×10^5 conidia mL^{-1}) of *Botrytis cinerea* (provided by N. Temme, Westfälische Wilhelms-Universität Munster). The strain, media, culture conditions, and pathogenicity assay were conducted according to Temme and Tudzynski (2009). Infected plants were incubated in a humidity chamber at 20°C under normal growth light conditions.

Statistical Analyses

The numerical data were subjected to statistical analysis using Student's *t* test, with statistical significance at the level of $P < 0.05$.

No new sequence data were generated in this study. If needed, the GenBank accession number for At4g15415 is NM_179059.

Supplemental Data

The following materials are available in the online version of this article.

Supplemental Figure S1. Amino acid sequence alignment of At4g15415 and At3g21650 and visual phenotypes of 4-week-old mutants deficient in PP2A-B′γ or PP2A-B′ζ.

Supplemental Table S1. Defense-related genes differentially expressed in *pp2a-b′γ* relative to wild-type plants under normal growth light conditions (130 μmol photons m^{-2} s^{-1}/22°C).

Supplemental Table S2. Adjustments in gene expression in knockdown *pp2a-b′γ* mutant plants grown under different light intensities.

ACKNOWLEDGMENTS

We thank Ina Schmitz-Thom (University of Munster) and Siri Tähtinen, Anna Lutz, Janina Stauffer, Ulla-Maija Suoranta, Marko Kaskinen, and Mika Keränen (University of Turku) for excellent technical assistance. We are grateful to Jouko Sandholm at the Cell Imaging Core of the Turku Center for Biotechnology, to the Finnish Microarray Center, to the Turku Proteomics Facility, and to CSC: Scientific Computing, Ltd., for providing technical support and the national license for GeneSpring. We thank the Salk Institute Genomic Analysis Laboratory for providing the sequence-indexed Arabidopsis T-DNA insertion mutants and full-length cDNA/open reading frame clones.

Received April 20, 2011; accepted May 11, 2011; published May 12, 2011.

LITERATURE CITED

Ahn CS, Han JA, Lee HS, Lee S, Pai HS (2011) The PP2A regulatory subunit Tap46, a component of the TOR signaling pathway, modulates growth and metabolism in plants. Plant Cell **23:** 185–209

Ali R, Ma W, Lemtiri-Chlieh F, Tsaltas D, Leng Q, von Bodman S, Berkowitz GA (2007) Death don't have no mercy and neither does calcium: *Arabidopsis* CYCLIC NUCLEOTIDE GATED CHANNEL2 and innate immunity. Plant Cell **19:** 1081–1095

Alonso JM, Stepanova AN, Leisse TJ, Kim CJ, Chen H, Shinn P, Stevenson DK, Zimmerman J, Barajas P, Cheuk R, et al (2003) Genome-wide insertional mutagenesis of Arabidopsis thaliana. Science **301:** 653–657

Alvarez ME, Nota F, Cambiagno DA (2010) Epigenetic control of plant immunity. Mol Plant Pathol **11:** 563–576

Amir R (2010) Current understanding of the factors regulating methionine content in vegetative tissues of higher plants. Amino Acids **39:** 917–931

Bechtold U, Richard O, Zamboni A, Gapper C, Geisler M, Pogson B, Karpinski S, Mullineaux PM (2008) Impact of chloroplastic- and extracellular-sourced ROS on high light-responsive gene expression in Arabidopsis. J Exp Bot **59:** 121–133

Benschop JJ, Mohammed S, O'Flaherty M, Heck AJR, Slijper M, Menke FLH (2007) Quantitative phosphoproteomics of early elicitor signaling in Arabidopsis. Mol Cell Proteomics **6:** 1198–1214

Bezhani S, Winter C, Hershman S, Wagner JD, Kennedy JF, Kwon CS, Pfluger J, Su Y, Wagner D (2007) Unique, shared, and redundant roles for the *Arabidopsis* SWI/SNF chromatin remodeling ATPases BRAHMA and SPLAYED. Plant Cell **19:** 403–416

Butt A, Mousley C, Morris K, Beynon J, Can C, Holub E, Greenberg JT, Buchanan-Wollaston V (1998) Differential expression of a senescence-enhanced metallothionein gene in Arabidopsis in response to isolates of *Peronospora parasitica* and *Pseudomonas syringae*. Plant J **16:** 209–221

Camilleri C, Azimzadeh J, Pastuglia M, Bellini C, Grandjean O, Bouchez D (2002) The *Arabidopsis TONNEAU2* gene encodes a putative novel protein phosphatase 2A regulatory subunit essential for the control of the cortical cytoskeleton. Plant Cell **14:** 833–845

Campell BR, Song Y, Posch TE, Cullis CA, Town CD (1992) Sequence and organization of 5S ribosomal RNA-encoding genes of Arabidopsis thaliana. Gene **112:** 225–228

Chang CC, Slesak I, Jordá L, Sotnikov A, Melzer M, Miszalski Z, Mullineaux PM, Parker JE, Karpinska B, Karpinski S (2009) Arabidopsis chloroplastic glutathione peroxidases play a role in cross talk between photooxidative stress and immune responses. Plant Physiol **150:** 670–683

Chang M, Wang B, Chen X, Wu R (1999) Molecular characterization of catalytic-subunit cDNA sequences encoding protein phosphatases 1 and 2A and study of their roles in the gibberellin-dependent Osamy-c expression in rice. Plant Mol Biol **39:** 105–115

Clarke JD, Volko SM, Ledford H, Ausubel FM, Dong X (2000) Roles of salicylic acid, jasmonic acid, and ethylene in cpr-induced resistance in *Arabidopsis*. Plant Cell **12:** 2175–2190

Clough SJ, Fengler KA, Yu IC, Lippok B, Smith RK Jr, Bent AF (2000) The Arabidopsis *dnd1* "*defense, no death*" gene encodes a mutated cyclic nucleotide-gated ion channel. Proc Natl Acad Sci USA **97:** 9323–9328

Damm B, Schmidt R, Willmitzer L (1989) Efficient transformation of *Arabidopsis thaliana* using direct gene transfer to protoplasts. Mol Gen Genet **217:** 6–12

Dat J, Vandenabeele S, Vranová E, Van Montagu M, Inzé D, Van Breusegem F (2000) Dual action of the active oxygen species during plant stress responses. Cell Mol Life Sci **57:** 779–795

Deal RB, Topp CN, McKinney EC, Meagher RB (2007) Repression of flowering in Arabidopsis requires activation of FLOWERING LOCUS C expression by the histone variant H2A.Z. Plant Cell **19:** 74–83

DeLong A (2006) Switching the flip: protein phosphatase roles in signaling pathways. Curr Opin Plant Biol **9:** 470–477

Dixon DP, Edwards R (2010) Roles for stress-inducible lambda glutathione transferases in flavonoid metabolism in plants as identified by ligand fishing. J Biol Chem **285:** 36322–36329

Durrant WE, Wang S, Dong X (2007) Arabidopsis SNI1 and RAD51D regulate both gene transcription and DNA recombination during the defense response. Proc Natl Acad Sci USA **104:** 4223–4227

Fan J, Crooks C, Creissen G, Hill L, Fairhurst S, Doerner P, Lamb C (2011) Pseudomonas sax genes overcome aliphatic isothiocyanate-mediated non-host resistance in Arabidopsis. Science **331:** 1185–1188

Farkas I, Dombrádi V, Miskei M, Szabados L, Koncz C (2007) Arabidopsis PPP family of serine/threonine phosphatases. Trends Plant Sci **12:** 169–176

Foyer CH, Noctor G (2009) Redox regulation in photosynthetic organisms: signaling, acclimation, and practical implications. Antioxid Redox Signal **11:** 861–905

Gadjev I, Vanderauwera S, Gechev TS, Laloi C, Minkov IN, Shulaev V, Apel K, Inzé D, Mittler R, Van Breusegem F (2006) Transcriptomic footprints disclose specificity of reactive oxygen species signaling in Arabidopsis. Plant Physiol **141:** 436–445

Griebel T, Zeier J (2008) Light regulation and daytime dependency of inducible plant defenses in Arabidopsis: phytochrome signaling controls systemic acquired resistance rather than local defense. Plant Physiol **147:** 790–801

He X, Anderson JC, del Pozo O, Gu YQ, Tang X, Martin GB (2004) Silencing of subfamily I of protein phosphatase 2A catalytic subunits results in activation of plant defense responses and localized cell death. Plant J **38:** 563–577

Heidari B, Matre P, Nemie-Feyissa D, Meyer C, Rognli OA, Møller SG, Lillo C (2011) Protein phosphatase 2A B55 and A regulatory subunits interact with nitrate reductase and are essential for nitrate reductase activation. Plant Physiol **156:** 165–172

Hirai MY, Sugiyama K, Sawada Y, Tohge T, Obayashi T, Suzuki A, Araki R, Sakurai N, Suzuki H, Aoki K, et al (2007) Omics-based identification of Arabidopsis Myb transcription factors regulating aliphatic glucosinolate biosynthesis. Proc Natl Acad Sci USA **104:** 6478–6483

Hoefgen R, Nikiforova VJ (2008) Metabolomics integrated with transcriptomics: assessing systems response to sulfur-deficiency stress. Physiol Plant **132:** 190–198

Jing H-C, Hebeler R, Oeljeklaus S, Sitek B, Stühler K, Meyer HE, Sturre MJG, Hille J, Warscheid B, Dijkwel PP (2008) Early leaf senescence is associated with an altered cellular redox balance in Arabidopsis *cpr5/old1* mutants. Plant Biol (Stuttg) (Suppl 1) **10:** 85–98

Jones AME, Bennett MH, Mansfield JW, Grant M (2006) Analysis of the defence phosphoproteome of *Arabidopsis thaliana* using differential mass tagging. Proteomics **6:** 4155–4165

Joo JH, Wang S, Chen JG, Jones AM, Fedoroff NV (2005) Different signaling and cell death roles of heterotrimeric G protein alpha and beta subunits in the *Arabidopsis* oxidative stress response to ozone. Plant Cell **17:** 957–970

Kachroo A, Lapchyk L, Fukushige H, Hildebrand D, Klessig D, Kachroo P (2003) Plastidial fatty acid signaling modulates salicylic acid- and jasmonic acid-mediated defense pathways in the *Arabidopsis ssi2* mutant. Plant Cell **15:** 2952–2965

Kangasjärvi S, Lepistö A, Hännikäinen K, Piippo M, Luomala EM, Aro EM, Rintamäki E (2008) Diverse roles for chloroplast stromal and thylakoid-bound ascorbate peroxidases in plant stress responses. Biochem J **412:** 275–285

Kangasjärvi S, Nurmi M, Tikkanen M, Aro EM (2009) Cell-specific mechanisms and systemic signalling as emerging themes in light acclimation of C3 plants. Plant Cell Environ **32:** 1230–1240

Kariola T, Brader G, Li J, Palva ET (2005) Chlorophyllase 1, a damage

control enzyme, affects the balance between defense pathways in plants. Plant Cell **17:** 282–294

Kiba A, Nishihara M, Tsukatani N, Nakatsuka T, Kato Y, Yamamura S (2005) A peroxiredoxin Q homolog from gentians is involved in both resistance against fungal disease and oxidative stress. Plant Cell Physiol **46:** 1007–1015

Kirik V, Bouyer D, Schöbinger U, Bechtold N, Herzog M, Bonneville JM, Hülskamp M (2001) CPR5 is involved in cell proliferation and cell death control and encodes a novel transmembrane protein. Curr Biol **11:** 1891–1895

König J, Lotte K, Plessow R, Brockhinke A, Baier M, Dietz KJ (2003) Reaction mechanism of plant 2-Cys peroxiredoxin: role of the C terminus and the quaternary structure. J Biol Chem **278:** 24409–24420

Kwak JM, Moon JH, Murata Y, Kuchitsu K, Leonhardt N, DeLong A, Schroeder JI (2002) Disruption of a guard cell-expressed protein phosphatase 2A regulatory subunit, *RCN1*, confers abscisic acid insensitivity in *Arabidopsis*. Plant Cell **14:** 2849–2861

Larsen PB, Cancel JD (2003) Enhanced ethylene responsiveness in the Arabidopsis *eer1* mutant results from a loss-of-function mutation in the protein phosphatase 2A A regulatory subunit, RCN1. Plant J **34:** 709–718

Lepistö A, Kangasjärvi S, Luomala EM, Brader G, Sipari N, Keränen M, Keinänen M, Rintamäki E (2009) Chloroplast NADPH-thioredoxin reductase interacts with photoperiodic development in Arabidopsis. Plant Physiol **149:** 1261–1276

Li X, Scuderi A, Letsou A, Virshup DM (2002) B56-associated protein phosphatase 2A is required for survival and protects from apoptosis in *Drosophila melanogaster*. Mol Cell Biol **22:** 3674–3684

Lim PO, Kim HJ, Nam HG (2007) Leaf senescence. Annu Rev Plant Biol **58:** 115–136

Liu G, Ji Y, Bhuiyan NH, Pilot G, Selvaraj G, Zou J, Wei Y (2010) Amino acid homeostasis modulates salicylic acid-associated redox status and defense responses in *Arabidopsis*. Plant Cell **22:** 3845–3863

Lohrig K, Müller B, Davydova J, Leister D, Wolters DA (2009) Phosphorylation site mapping of soluble proteins: bioinformatical filtering reveals potential plastidic phosphoproteins in Arabidopsis thaliana. Planta **229:** 1123–1134

Lorrain S, Vailleau F, Balagué C, Roby D (2003) Lesion mimic mutants: keys for deciphering cell death and defense pathways in plants? Trends Plant Sci **8:** 263–271

Mateo A, Funck D, Mühlenbock P, Kular B, Mullineaux PM, Karpinski S (2006) Controlled levels of salicylic acid are required for optimal photosynthesis and redox homeostasis. J Exp Bot **57:** 1795–1807

Mateo A, Mühlenbock P, Rustérucci C, Chang CC, Miszalski Z, Karpinska B, Parker JE, Mullineaux PM, Karpinski S (2004) LESION SIMULATING DISEASE 1 is required for acclimation to conditions that promote excess excitation energy. Plant Physiol **136:** 2818–2830

Matre P, Meyer C, Lillo C (2009) Diversity in subcellular targeting of the PP2A B′eta subfamily members. Planta **230:** 935–945

Moeder W, Del Pozo O, Navarre DA, Martin GB, Klessig DF (2007) Aconitase plays a role in regulating resistance to oxidative stress and cell death in Arabidopsis and Nicotiana benthamiana. Plant Mol Biol **63:** 273–287

Moffatt BA, Weretilnyk EA (2001) Sustaining S-adenosyl-L-methionine-dependent methyltransferase activity in plant cells. Physiol Plant **113:** 435–442

Monroy AF, Sangwan V, Dhindsa RS (1998) Low temperature signal transduction during cold acclimation: protein phosphatase 2A as an early target for cold-inactivation. Plant J **13:** 653–660

Mühlenbock P, Szechynska-Hebda M, Plaszczyca M, Baudo M, Mateo A, Mullineaux PM, Parker JE, Karpinska B, Karpinski S (2008) Chloroplast signaling and LESION SIMULATING DISEASE1 regulate crosstalk between light acclimation and immunity in *Arabidopsis*. Plant Cell **20:** 2339–2356

Negrutiu I, Shillito R, Potrykus I, Biasini G, Sala F (1987) Hybrid genes in the analysis of transformation conditions. Plant Mol Biol **8:** 363–373

Nühse TS, Bottrill AR, Jones AME, Peck SC (2007) Quantitative phosphoproteomic analysis of plasma membrane proteins reveals regulatory mechanisms of plant innate immune responses. Plant J **51:** 931–940

Pavet V, Quintero C, Cecchini NM, Rosa AL, Alvarez ME (2006) Arabidopsis displays centromeric DNA hypomethylation and cytological alterations of heterochromatin upon attack by Pseudomonas syringae. Mol Plant Microbe Interact **19:** 577–587

Peltier JB, Cai Y, Sun Q, Zabrouskov V, Giacomelli L, Rudella A, Ytterberg AJ, Rutschow H, van Wijk KJ (2006) The oligomeric stromal proteome of Arabidopsis thaliana chloroplasts. Mol Cell Proteomics **5:** 114–133

Penninckx IAMA, Thomma BPHJ, Buchala A, Métraux JP, Broekaert WF (1998) Concomitant activation of jasmonate and ethylene response pathways is required for induction of a plant defensin gene in *Arabidopsis*. Plant Cell **10:** 2103–2113

Pernas M, García-Casado G, Rojo E, Solano R, Sánchez-Serrano JJ (2007) A protein phosphatase 2A catalytic subunit is a negative regulator of abscisic acid signalling. Plant J **51:** 763–778

Piippo M, Allahverdiyeva Y, Paakkarinen V, Suoranta UM, Battchikova N, Aro EM (2006) Chloroplast-mediated regulation of nuclear genes in *Arabidopsis thaliana* in the absence of light stress. Physiol Genomics **25:** 142–152

Qiu JL, Zhou L, Yun BW, Nielsen HB, Fiil BK, Petersen K, Mackinlay J, Loake GJ, Mundy J, Morris PC (2008) Arabidopsis mitogen-activated protein kinase kinases MKK1 and MKK2 have overlapping functions in defense signaling mediated by MEKK1, MPK4, and MKS1. Plant Physiol **148:** 212–222

Queval G, Issakidis-Bourguet E, Hoeberichts FA, Vandorpe M, Gakière B, Vanacker H, Miginiac-Maslow M, Van Breusegem F, Noctor G (2007) Conditional oxidative stress responses in the Arabidopsis photorespiratory mutant *cat2* demonstrate that redox state is a key modulator of daylength-dependent gene expression, and define photoperiod as a crucial factor in the regulation of H_2O_2-induced cell death. Plant J **52:** 640–657

Quirino BF, Normanly J, Amasino RM (1999) Diverse range of gene activity during *Arabidopsis thaliana* leaf senescence includes pathogen-independent induction of defense-related genes. Plant Mol Biol **40:** 267–278

Rashotte AM, DeLong A, Muday GK (2001) Genetic and chemical reductions in protein phosphatase activity alter auxin transport, gravity response, and lateral root growth. Plant Cell **13:** 1683–1697

Rocha PS, Sheikh M, Melchiorre R, Fagard M, Boutet S, Loach R, Moffatt B, Wagner C, Vaucheret H, Furner I (2005) The *Arabidopsis* HOMOLOGY-DEPENDENT GENE SILENCING1 gene codes for an S-adenosyl-L-homocysteine hydrolase required for DNA methylation-dependent gene silencing. Plant Cell **17:** 404–417

Rojo E, Titarenko E, León J, Berger S, Vancanneyt G, Sánchez-Serrano JJ (1998) Reversible protein phosphorylation regulates jasmonic acid-dependent and -independent wound signal transduction pathways in *Arabidopsis thaliana*. Plant J **13:** 153–165

Rokka A, Suorsa M, Saleem A, Battchikova N, Aro EM (2005) Synthesis and assembly of thylakoid protein complexes: multiple assembly steps of photosystem II. Biochem J **388:** 159–168

Saito N, Munemasa S, Nakamura Y, Shimoishi Y, Mori IC, Murata Y (2008) Roles of RCN1, regulatory A subunit of protein phosphatase 2A, in methyl jasmonate signaling and signal crosstalk between methyl jasmonate and abscisic acid. Plant Cell Physiol **49:** 1396–1401

Schmelz EA, Engelberth J, Alborn HT, O'Donnell P, Sammons M, Toshima H, Tumlinson JH III (2003) Simultaneous analysis of phytohormones, phytotoxins, and volatile organic compounds in plants. Proc Natl Acad Sci USA **100:** 10552–10557

Schweighofer A, Kazanaviciute V, Scheikl E, Teige M, Doczi R, Hirt H, Schwanninger M, Kant M, Schuurink R, Mauch F, et al (2007) The PP2C-type phosphatase AP2C1, which negatively regulates MPK4 and MPK6, modulates innate immunity, jasmonic acid, and ethylene levels in *Arabidopsis*. Plant Cell **19:** 2213–2224

Shirzadian-Khorramabad R, Jing HC, Everts GE, Schippers JH, Hille J, Dijkwel PP (2010) A mutation in the cytosolic O-acetylserine (thiol) lyase induces a genome-dependent early leaf death phenotype in Arabidopsis. BMC Plant Biol **10:** 80

Slaymaker DH, Navarre DA, Clark D, del Pozo O, Martin GB, Klessig DF (2002) The tobacco salicylic acid-binding protein 3 (SABP3) is the chloroplast carbonic anhydrase, which exhibits antioxidant activity and plays a role in the hypersensitive defense response. Proc Natl Acad Sci USA **99:** 11640–11645

Smith AP, Nourizadeh SD, Peer WA, Xu J, Bandyopadhyay A, Murphy AS, Goldsbrough PB (2003) Arabidopsis AtGSTF2 is regulated by ethylene and auxin, and encodes a glutathione S-transferase that interacts with flavonoids. Plant J **36:** 433–442

Tang W, Yuan M, Wang R, Yang Y, Wang C, Oses-Prieto JA, Kim TW, Zhou HW, Deng Z, Gampala SS, et al (2011) PP2A activates brassinosteroid-responsive gene expression and plant growth by dephosphorylating BZR1. Nat Cell Biol **13:** 124–131

Temme N, Tudzynski P (2009) Does *Botrytis cinerea* ignore H_2O_2-induced

oxidative stress during infection? Characterization of *Botrytis* activator protein 1. Mol Plant Microbe Interact **22:** 987–998

Tena G, Asai T, Chiu WL, Sheen J (2001) Plant mitogen-activated protein kinase signaling cascades. Curr Opin Plant Biol **4:** 392–400

Thordal-Christensen H, Zhang Z, Wei Y, Collinge DB (1997) Subcellular localization of H_2O_2 in plants: H_2O_2 accumulation in papillae and hypersensitive response during the barley-powdery mildew interaction. Plant J **11:** 1187–1194

Tseng TS, Briggs WR (2010) The *Arabidopsis rcn1-1* mutation impairs dephosphorylation of Phot2, resulting in enhanced blue light responses. Plant Cell **22:** 392–402

Weigel D, Glazebrook J (2002) Arabidopsis: A Laboratory Manual. Cold Spring Harbor Laboratory Press, Cold Spring Harbor, NY

Xing T, Ouellet T, Miki BL (2002) Towards genomic and proteomic studies of protein phosphorylation in plant-pathogen interactions. Trends Plant Sci **7:** 224–230

Yamada K, Lim J, Dale JM, Chen H, Shinn P, Palm CJ, Southwick AM, Wu HC, Kim C, Nguyen M, et al (2003) Empirical analysis of transcriptional activity in the Arabidopsis genome. Science **302:** 842–846

Yoshida S, Ito M, Nishida I, Watanabe A (2002) Identification of a novel gene HYS1/CPR5 that has a repressive role in the induction of leaf senescence and pathogen-defence responses in *Arabidopsis thaliana*. Plant J **29:** 427–437

Yu IC, Parker J, Bent AF (1998) Gene-for-gene disease resistance without the hypersensitive response in Arabidopsis *dnd1* mutant. Proc Natl Acad Sci USA **95:** 7819–7824